

# Design and analysis of ADER-type schemes for model advection-diffusion-reaction equations

S. Busto<sup>1</sup>, E. F. Toro<sup>2</sup>, M. E. Vázquez-Cendón<sup>3</sup>

<sup>(1,3)</sup> *Departamento de Matemática Aplicada, Universidade de Santiago de Compostela. Facultad de Matemáticas, ES-15782 Santiago de Compostela, Spain*

<sup>(2)</sup> *Department of Civil, Environmental and Mechanical Engineering, University of Trento, Via Mesiano 77, 38123 Trento, Italy*

---

## Abstract

We construct, analyse and assess various schemes of second order of accuracy in space and time for model advection-diffusion-reaction differential equations. The constructed schemes are meant to be of practical use in solving industrial problems and are derived following two related approaches, namely ADER and MUSCL-Hancock. Detailed analysis of linear stability and local truncation error are carried out. In addition, the schemes are implemented and assessed for various test problems. Empirical convergence rate studies confirm the theoretically expected accuracy in both space and time.

*Keywords:* Advection-diffusion-reaction equations; finite volume method; ADER approach; MUSCL-Hancock method; local truncation error; linear stability; empirical convergence rates.

---

## 1 Introduction

Advection-diffusion-reaction equations are present in a wide range of physical/biological problems. The Navier-Stokes equations are a prominent example, which constitute a major focus for the development of numerical methods of practical use to the scientific community. A classical and successful approach for solving the aforementioned and related equations are finite volume methods (e.g. see [37], [2], [14], [24] and references herein).

A motivation of this paper concerns the simulation of low Mach number flows in a turbulent regime. The phenomenon can be represented by the Navier-Stokes equations coupled to a RANS  $k - \varepsilon$  turbulent model, see [1]. The approach introduces turbulent viscosity, which is typically computed by solving an additional pair of advection-diffusion-reaction equations, that is equations for the turbulent kinetic energy and dissipation rate. One issue here is the time dependency of the viscous term. This requires the use of methods that are at least second-order accurate in space and time for all terms involved. In practice, it is often the case that the numerical methods used are of low order of accuracy. Typically, methods may be of second order in space but only first order in time, or may be second order in both space and time but only for some of the terms in the equations. For diffusion equations a popular choice is the second-order Crank-Nicolson method, see [29]. The accuracy for reaction terms, coupled to the remaining terms of the equations, is usually sacrificed, resulting in overall low order of accuracy.

For advection equations, several approaches for constructing high-order methods have been put forward. A classical example is the Lax-Wendroff scheme [22], [23]. This scheme is linear in the sense of Godunov [15] and thus oscillatory, according to Godunov's theorem [15]. We note that the oscillatory nature remains so even when (physical) viscous terms are added. A major step forward in this direction was the work of Kolgan [21], who introduced, for the first time, a numerical scheme that circumvents Godunov's theorem, via the construction of a non-linear scheme using non-linear reconstructions (limited slopes), see [3] and [7] for further details. Since then, many more works have appeared in the literature, reporting schemes, such as Total Variation Diminishing Methods (TVD) and Flux Limiter Methods (see, for instance, [46], [47] and [31]). Comprehensive reviews are found in [37] and [24], for example.

---

<sup>1</sup>saray.busto@usc.es

<sup>2</sup>eleuterio.toro@unitn.it

<sup>3</sup>elena.vazquez.cendon@usc.es

More advanced non-linear methods for advection dominated problems include the semi-discrete ENO, see [16], and WENO, see [29] and [25], approaches. See also the method of Harten and collaborators [16], which is a fully discrete high-order scheme. In [6], this scheme was called the HEOC scheme, and was re-interpreted in terms of the solution of a generalised Riemann problem, solved in a particular way. In fact, it is easily shown that the HEOC scheme is a generalisation of the MUSCL-Hancock method, see [46].

The ADER approach, first put forward in [40], is also a fully discrete approach that relies on non-linear reconstructions and the solution of the generalised Riemann problem, to any order of accuracy. The resulting schemes are arbitrarily accurate in both space and time in the sense that they have no theoretical accuracy barrier. An introduction to ADER schemes is found in Chapters 19 and 20 of [37]. Further developments and applications are found, for example, in [34], [38], [45], [35], [33], [36], [10], [32], [44], [5], [49], [4], [20], [43], [26], [27], [17], [8], [9], [28], [12], [13], [11], [18].

The aim of this paper is to develop finite volume schemes of second-order in time and space to solve the advection-diffusion-reaction equation, admitting space and time dependent diffusion coefficients. We follow the ADER and MUSCL-Hancock methodologies and compare both approaches. Detailed analysis, such as linear stability and accuracy in the sense of local truncation error is lacking for these methodologies applied to advection-diffusion-reaction equations. The main objective of this paper is precisely to carry out detailed stability and accuracy analysis of these methods. Moreover, to determine the stability region and a new graphical methodology is introduced.

The outline of this paper is as follows. In Section 2 the advection-diffusion-reaction equation is introduced. Section 3 is devoted to the development of a numerical scheme for the advection-diffusion-reaction equation. The ADER approach is adopted to approximate linear advection-reaction equations and is modified to account for the diffusion term. The methodology developed for the ADER scheme to treat source-term like terms is applied to the MUSCL-Hancock method in Section 4. In Section 5, we conduct a linear stability analysis of the schemes. Section 6 is devoted to the study of empirical convergence rates of the scheme. Conclusions are drawn in Section 7 and A is devoted to the analysis of local truncation errors of the proposed schemes.

## 2 The advection-diffusion-reaction equation

The advection-diffusion-reaction equation reads

$$\partial_t q(x, t) + \lambda \partial_x q(x, t) = \partial_x (\alpha \partial_x q)(x, t) + \beta q(x, t) \quad (1)$$

where  $q(x, t)$  is the conservative variable;  $x, t$  are the spatial and temporal independent variables;  $\lambda$  is the characteristic speed;  $\alpha(x, t)$  is the diffusion coefficient, a prescribed function; and  $\beta$  is the coefficient of the reaction term (source term).

In order to solve equation (1) we work in the finite volume framework. To start with, we consider the control volume  $V = [x_{i-\frac{1}{2}}, x_{i+\frac{1}{2}}] \times [t^n, t^{n+1}]$  in the  $x - t$  plane, of dimensions,  $\Delta x = x_{i+\frac{1}{2}} - x_{i-\frac{1}{2}}$ ,  $\Delta t = t^{n+1} - t^n$ . Then, exact integration of equation (1) in the control volume  $V$  gives

$$\begin{aligned} & \frac{1}{\Delta x} \int_{x_{i-\frac{1}{2}}}^{x_{i+\frac{1}{2}}} (q(x, t^{n+1}) - q(x, t^n)) dx + \frac{1}{\Delta x} \int_{t^n}^{t^{n+1}} (f(q(x_{i+\frac{1}{2}}, t)) - f(q(x_{i-\frac{1}{2}}, t))) dt \\ &= \frac{1}{\Delta x} \int_{x_{i-\frac{1}{2}}}^{x_{i+\frac{1}{2}}} \left( \int_{t^n}^{t^{n+1}} \partial_x (\alpha \partial_x q)(x, t) dx \right) dt + \frac{1}{\Delta x} \int_{x_{i-\frac{1}{2}}}^{x_{i+\frac{1}{2}}} \left( \int_{t^n}^{t^{n+1}} \beta q(x, t) dx \right) dt. \end{aligned}$$

Introducing the notation

$$\begin{aligned} q_i^{n+1} &= \frac{1}{\Delta x} \int_{x_{i-\frac{1}{2}}}^{x_{i+\frac{1}{2}}} q(x, t^{n+1}) dx, & q_i^n &= \frac{1}{\Delta x} \int_{x_{i-\frac{1}{2}}}^{x_{i+\frac{1}{2}}} q(x, t^n) dx, \\ f_{i+\frac{1}{2}}^n &= \frac{1}{\Delta t} \int_{t^n}^{t^{n+1}} f(q(x_{i+\frac{1}{2}}, t)) dt, & f_{i-\frac{1}{2}}^n &= \frac{1}{\Delta t} \int_{t^n}^{t^{n+1}} f(q(x_{i-\frac{1}{2}}, t)) dt, \end{aligned}$$

$$g_i^n = \frac{1}{\Delta t \Delta x} \int_{x_{i-\frac{1}{2}}}^{x_{i+\frac{1}{2}}} \left( \int_{t^n}^{t^{n+1}} \partial_x (\alpha \partial_x q)(x, t) dx \right) dt,$$

$$s_i^n = \frac{1}{\Delta t \Delta x} \int_{x_{i-\frac{1}{2}}}^{x_{i+\frac{1}{2}}} \left( \int_{t^n}^{t^{n+1}} \beta q(x, t) dx \right) dt,$$

we arrive at the exact relation

$$q_i^{n+1} = q_i^n - \frac{\Delta t}{\Delta x} \left( f_{i+\frac{1}{2}}^n - f_{i-\frac{1}{2}}^n \right) + \Delta t g_i^n + \Delta t s_i^n. \quad (2)$$

Thus, we can construct a numerical method to find the solution of (1) at time  $t^{n+1}$  by interpreting (2) in an approximate manner, that is by approximating the integrals in (2). We analyse two different approaches for computing them, the ADER and the MUSCL-Hancock methodologies. For the sake of simplicity, we will use the same notation for the approximate values than for the exact values of the integrals in (2). It is appropriate to remark that the integral  $g_i^n$  could be further integrated to yield corresponding expressions for viscous numerical fluxes.

### 3 The ADER approach

The Arbitrary high order DERivative Riemann problem (ADER) approach was first put forward in [40] for the linear advection equation in one and three space dimensions. In this section, we introduce a modification of the ADER approach to solve the advection-diffusion-reaction equation. The proposed method includes the following steps:

**Step 1.** Polynomial reconstruction. Following [40], we consider a reconstruction of the data in terms of first-degree polynomials of the form

$$p_i(x) = q_i^n + \Delta_i(x - x_i),$$

where  $\Delta_i$  denotes the spatial derivative of  $q(x, t)$  at time  $t^n$  in volume  $i$  (or an approximation) for  $i = 1, 2, \dots, M$ , where  $M$  is the total number of finite volumes. In the present paper, we only consider centred slopes, that is

$$\Delta_i = \frac{q_{i+1}^n - q_{i-1}^n}{2\Delta x}, \quad (3)$$

which, as proved in A, will provide a scheme of second order accuracy in space and time. We note however that the resulting schemes will be linear and hence oscillatory in the presence of large spatial gradients.

**Step 2.** Solution of the generalized Riemann problem (GRP). To construct the numerical flux the following generalizations of the Classical Riemann Problem are made. On the one hand, the initial condition is assumed to be a piecewise first-degree polynomial. On the other hand, the partial differential equation accounts for the diffusion and reaction terms. That leads to the problem

$$\begin{cases} \partial_t q(x, t) + \lambda \partial_x q(x, t) = \partial_x (\alpha \partial_x q)(x, t) + \beta q(x, t), \\ q(x, 0) = \begin{cases} p_i(x), & x < 0, \\ p_{i+1}(x), & x > 0. \end{cases} \end{cases} \quad (4)$$

**Step 3.** Source term and diffusion term. These terms are computed by approximating the integrals by the mid-point rule in both space and time.

In the following sections we will develop the last two steps.

### 3.1 Step 2. Solution of the generalized Riemann problem

For ease of presentation, two different cases for the diffusion term will be considered: zero diffusion term and a space and time dependent diffusion coefficient.

#### 3.1.1 Numerical flux without diffusion

Expressing the solution of the GRP at the interface as a Taylor series expansion in time we have

$$\bar{q}_{i+\frac{1}{2}} = q(0, 0_+) + \tau \partial_t q(0, 0_+). \quad (5)$$

We find the solution of (4) as given by two terms. One being the solution of a classical Riemann problem,  $q(0, 0_+)$ , and the other as given by the high order term,  $\tau \partial_t q(0, 0_+)$ .

The solution of the classical Riemann problem

$$\begin{cases} \partial_t q(x, t) + \lambda \partial_x q(x, t) = 0, \\ q(x, 0) = \begin{cases} q_i^n + \frac{1}{2} \Delta x \Delta_i, & x < 0, \\ q_{i+1}^n - \frac{1}{2} \Delta x \Delta_{i+1}, & x > 0, \end{cases} \end{cases}$$

is

$$q(x, t) = d_{i+\frac{1}{2}}^{(0)}(x/t) = \begin{cases} q_i^n + \frac{1}{2} \Delta x \Delta_i, & \frac{x}{t} < \lambda, \\ q_{i+1}^n - \frac{1}{2} \Delta x \Delta_{i+1}, & \frac{x}{t} > \lambda, \end{cases}$$

hence, the solution for  $\frac{x}{t} = 0$  is given by

$$q(0, 0_+) = d_{i+\frac{1}{2}}^{(0)}(0) = \begin{cases} q_i^n + \frac{1}{2} \Delta x \Delta_i, & \lambda > 0, \\ q_{i+1}^n - \frac{1}{2} \Delta x \Delta_{i+1}, & \lambda < 0. \end{cases} \quad (6)$$

On the other hand, regarding Cauchy-Kovalevskaya procedure and assuming a zero diffusion term, it is verified

$$\partial_t q(x, t) = -\lambda \partial_x q(x, t) + \beta q(x, t),$$

thus, we can express (5) in terms of spatial derivatives

$$\bar{q}_{i+\frac{1}{2}} = q(0, 0_+) + \tau [-\lambda \partial_x q(0, 0_+) + \beta q(0, 0_+)]. \quad (7)$$

It is easy to show that the following evolution equation for the spatial derivative of the conservative variable is valid

$$\partial_t (\partial_x q(x, t)) + \lambda \partial_x^{(2)} q(x, t) = \beta \partial_x q(x, t). \quad (8)$$

Neglecting the source term, a new classical Riemann problem can be set for the spatial gradient

$$\begin{cases} \partial_t (\partial_x q(x, t)) + \lambda \partial_x^{(2)} q(x, t) = 0, \\ \partial_x q(x, 0) = \begin{cases} \Delta_i, & x < 0, \\ \Delta_{i+1}, & x > 0. \end{cases} \end{cases} \quad (9)$$

Its solution is

$$\partial_x q(x, t) = d_{i+\frac{1}{2}}^{(1)} \left( \frac{x}{t} \right) = \begin{cases} \Delta_i, & \frac{x}{t} < \lambda, \\ \Delta_{i+1}, & \frac{x}{t} > \lambda, \end{cases} \quad (10)$$

and

$$\partial_x q(0, 0_+) = d_{i+\frac{1}{2}}^{(1)}(0) = \begin{cases} \Delta_i, & \lambda > 0, \\ \Delta_{i+1}, & \lambda < 0, \end{cases} \quad (11)$$

is the solution at  $\frac{x}{t} = 0$ .

Then, from (6) and (11), the sought complete solution reads

$$\begin{aligned} \bar{q}_{i+\frac{1}{2}} &= q(0, 0_+) + \tau \partial_t q(0, 0_+) \\ &= \begin{cases} q_i^n + \frac{1}{2} \Delta x \Delta_i + \tau [-\lambda \Delta_i + \beta (q_i^n + \frac{1}{2} \Delta x \Delta_i)] & \lambda > 0, \\ q_{i+1}^n - \frac{1}{2} \Delta x \Delta_{i+1} + \tau [-\lambda \Delta_{i+1} + \beta (q_{i+1}^n - \frac{1}{2} \Delta x \Delta_{i+1})] & \lambda < 0. \end{cases} \end{aligned} \quad (12)$$

Performing exact integration, or equivalently applying the mid-point rule with  $\tau = \frac{1}{2} \Delta t$ , we obtain the numerical flux,

$$f_{i+\frac{1}{2}} = \begin{cases} \lambda \left\{ q_i^n + \frac{1}{2} \Delta x \Delta_i + \frac{\Delta t}{2} [-\lambda \Delta_i + \beta (q_i^n + \frac{1}{2} \Delta x \Delta_i)] \right\} & \lambda > 0, \\ \lambda \left\{ q_{i+1}^n - \frac{1}{2} \Delta x \Delta_{i+1} + \frac{\Delta t}{2} [-\lambda \Delta_{i+1} + \beta (q_{i+1}^n - \frac{1}{2} \Delta x \Delta_{i+1})] \right\} & \lambda < 0. \end{cases}$$

### 3.1.2 Numerical flux with diffusion

In order to treat the diffusion term we adopt the following strategy. The diffusion term is regarded as a source term but is introduced in the Cauchy-Kovalevskaya procedure and is evaluated in an upwind fashion. The upwinding of the diffusion term can be justified because in the case of constant diffusion coefficient  $\alpha$ , the second derivative of the solution  $q(x, y)$  of the linear advection equation, in fact any order derivative, obeys identically the same linear advection equation. Hence we can pose and solve a classical Riemann problem for these spatial derivatives leading effectively to *upwinding the diffusion term*.

The Cauchy-Kovalevskaya procedure used in the Taylor series expansion in time for the solution of the GRP,

$$\bar{q}_{i+\frac{1}{2}} = q(0, 0_+) + \tau \partial_t q(0, 0_+),$$

gives

$$\bar{q}_{i+\frac{1}{2}} = q(0, 0_+) + \tau [-\lambda \partial_x q(0, 0_+) + \partial_x (\alpha \partial_x q)(0, 0_+) + \beta q(0, 0_+)].$$

As anticipated previously, the term  $\partial_x (\alpha \partial_x q)(0, 0_+)$  is approximated in a central difference fashion as follows

$$\partial_x (\alpha \partial_x q)(0, 0_+) = \frac{1}{\Delta x^2} \left[ \alpha_{i+\frac{1}{2}} (q_{i+1}^n - q_i^n) - \alpha_{i-\frac{1}{2}} (q_i^n - q_{i-1}^n) \right]. \quad (13)$$

The choice made for approximating the diffusion term in this manner is motivated by the fact that in our existing 3D Navier-Stokes code in development this term will be computed by solving a pair of advection-diffusion-reaction equations.

For notational convenience we set  $(\Delta\alpha\Delta)_i = \partial_x(\alpha\partial_x q)(0, 0_+)$ . Integrating, the numerical flux results

$$f_{i+\frac{1}{2}} = \begin{cases} \lambda \left\{ q_i^n + \frac{1}{2}\Delta x\Delta_i + \frac{\Delta t}{2} [-\lambda\Delta_i + \beta(q_i^n + \frac{1}{2}\Delta x\Delta_i) + (\Delta\alpha\Delta)_i] \right\} & \lambda > 0, \\ \lambda \left\{ q_{i+1}^n - \frac{1}{2}\Delta x\Delta_{i+1} + \frac{\Delta t}{2} [-\lambda\Delta_{i+1} + \beta(q_{i+1}^n - \frac{1}{2}\Delta x\Delta_{i+1}) + (\Delta\alpha\Delta)_{i+1}] \right\} & \lambda < 0. \end{cases} \quad (14)$$

**Remark 1.** From now on, we will focus on the development and analysis of the schemes for  $\lambda > 0$ . The results for  $\lambda < 0$  can be obtained similarly.

**Remark 2.** The whole scheme can be derived from the finite volume framework, resulting in an intercell numerical flux with two terms, one for the advection and one for the diffusion, see [42] and [39]. However, it is worth mentioning that through an appropriated choice of the approximation for the slopes it will result in the same numerical scheme than the one proposed in this paper.

Furthermore, our motivation is to couple the numerical method developed in this paper to an existing three-dimensional Navier-Stokes, see [1], to this end the approach proposed here turns out to be very convenient and achieves the order of accuracy sought.

### 3.2 Step 3. Approximation of the diffusion and reaction terms

Recall that second-order approximations to the integrals defining the finite volume method can be obtained via the mid-point rule approximation, see [37]. This requires an approximation at the centre of the volume at the half time, which is achieved by a Taylor expansion and the use of the Cauchy-Kovalevskaya procedure, namely

$$\overline{q_i^n} = q_i^n + \tau(-\lambda\Delta_i + (\Delta\alpha\Delta)_i + \beta q_i^n).$$

#### 3.3 Step 3.1. Diffusion term

The approximation of the diffusion term becomes

$$\overline{(\Delta\alpha\Delta)_i} = \frac{\overline{\alpha_{i+\frac{1}{2}}^n} \overline{\Delta_{i+\frac{1}{2}}} - \overline{\alpha_{i-\frac{1}{2}}^n} \overline{\Delta_{i-\frac{1}{2}}}}{\Delta x} = \frac{1}{\Delta x^2} \left[ \overline{\alpha_{i+\frac{1}{2}}^n} (\overline{q_{i+1}^n} - \overline{q_i^n}) - \overline{\alpha_{i-\frac{1}{2}}^n} (\overline{q_i^n} - \overline{q_{i-1}^n}) \right],$$

that is

$$\begin{aligned} \overline{(\Delta\alpha\Delta)_i} = & \frac{1}{\Delta x^2} \left\{ \left[ \alpha_{i+\frac{1}{2}}^n + \frac{\Delta t}{2} \partial_t \alpha_{i+\frac{1}{2}} \right] \left[ q_{i+1}^n - q_i^n + \frac{\Delta t}{2} (-\lambda(\Delta_{i+1} - \Delta_i) \right. \right. \\ & \left. \left. + (\Delta\alpha\Delta)_{i+1} - (\Delta\alpha\Delta)_i + \beta(q_{i+1}^n - q_i^n) \right] \right. \\ & \left. + \left[ \alpha_{i-\frac{1}{2}}^n + \frac{\Delta t}{2} \partial_t \alpha_{i-\frac{1}{2}} \right] \left[ q_i^n - q_{i-1}^n + \frac{\Delta t}{2} (-\lambda(\Delta_{i-1} - \Delta_i) \right. \right. \\ & \left. \left. + (\Delta\alpha\Delta)_{i-1} - (\Delta\alpha\Delta)_i + \beta(q_{i-1}^n - q_i^n) \right] \right\} \end{aligned} \quad (15)$$

where the time derivative of the viscous coefficient can be computed as

$$\partial_t \alpha_{i+\frac{1}{2}} \approx \frac{1}{2} \left( \frac{\alpha_{i+1}^n - \alpha_{i+1}^{n-1}}{\Delta t} + \frac{\alpha_i^n - \alpha_i^{n-1}}{\Delta t} \right). \quad (16)$$

If  $\alpha$  is a function depending on conservative variables (which would be the case, for example, of the viscous term for turbulent Navier-Stokes equations), we can also use the Cauchy-Kovalevskaya procedure.

### 3.3.1 Step 3.2. Numerical source

Lumping together the contributions of the reactive and diffusion terms we get a *numerical source* term as follows

$$s_i = \beta \bar{q}_i = \beta \left[ q_i + \frac{\Delta t}{2} (-\lambda \Delta_i + (\Delta \alpha \Delta)_i + \beta q_i) \right]. \quad (17)$$

Gathering (14), (15) and (17), the numerical scheme for the advection-diffusion-reaction equation, with  $\lambda > 0$ , reads

$$\begin{aligned} q_i^{n+1} = & q_i^n - \frac{\lambda \Delta t}{\Delta x} \left\{ q_i^n + \frac{1}{2} \Delta x \Delta_i + \frac{\Delta t}{2} \left[ -\lambda \Delta_i + \beta \left( q_i^n + \frac{1}{2} \Delta x \Delta_i \right) + (\Delta \alpha \Delta)_i \right] \right. \\ & \left. - q_{i-1}^n - \frac{1}{2} \Delta x \Delta_{i-1} - \frac{\Delta t}{2} \left[ -\lambda \Delta_{i-1} + \beta \left( q_{i-1}^n + \frac{1}{2} \Delta x \Delta_{i-1} \right) + (\Delta \alpha \Delta)_{i-1} \right] \right\} \\ & + \frac{\Delta t}{\Delta x^2} \left\{ \left[ \alpha_{i+\frac{1}{2}}^n + \frac{\Delta t}{2} \partial_t \alpha_{i+\frac{1}{2}} \right] \left[ q_{i+1}^n - q_i^n + \frac{\Delta t}{2} (-\lambda (\Delta_{i+1} - \Delta_i) \right. \right. \\ & \left. \left. + (\Delta \alpha \Delta)_{i+1} - (\Delta \alpha \Delta)_i + \beta (q_{i+1}^n - q_i^n) \right] \right. \\ & \left. + \left[ \alpha_{i-\frac{1}{2}}^n + \frac{\Delta t}{2} \partial_t \alpha_{i-\frac{1}{2}} \right] \left[ q_{i-1}^n - q_i^n + \frac{\Delta t}{2} (-\lambda (\Delta_{i-1} - \Delta_i) \right. \right. \\ & \left. \left. + (\Delta \alpha \Delta)_{i-1} - (\Delta \alpha \Delta)_i + \beta (q_{i-1}^n - q_i^n) \right] \right\} \\ & + \beta \Delta t \left[ q_i + \frac{\Delta t}{2} (-\lambda \Delta_i + (\Delta \alpha \Delta)_i + \beta q_i) \right]. \end{aligned} \quad (18)$$

Finally, taking into account the centred approach of the slopes, (3) and (13), one obtains

$$\begin{aligned} q_i^{n+1} = & q_i^n - c \left\{ \frac{2+r}{2} (q_i^n - q_{i-1}^n) + \frac{2-2c+r}{8} (q_{i+1}^n - q_i^n - q_{i-1}^n + q_{i-2}^n) \right. \\ & \left. + \frac{\Delta t}{2\Delta x^2} \left[ \alpha_{i+\frac{1}{2}}^n (q_{i+1}^n - q_i^n) - 2\alpha_{i-\frac{1}{2}}^n (q_i^n - q_{i-1}^n) + \alpha_{i-\frac{3}{2}}^n (q_{i-1}^n - q_{i-2}^n) \right] \right\} \\ & + \frac{\Delta t}{\Delta x^2} \left\{ \left[ \alpha_{i+\frac{1}{2}}^n + \frac{\Delta t}{2} \partial_t \alpha_{i+\frac{1}{2}} \right] \left[ \frac{2+r}{2} (q_{i+1}^n - q_i^n) - \frac{c}{4} (q_{i+2}^n - q_{i+1}^n \right. \right. \\ & \left. \left. - q_i^n + q_{i-1}^n) + \frac{\Delta t}{2\Delta x^2} \left( \alpha_{i+\frac{3}{2}}^n (q_{i+2}^n - q_{i+1}^n) - 2\alpha_{i+\frac{1}{2}}^n (q_{i+1}^n - q_i^n) \right. \right. \right. \\ & \left. \left. + \alpha_{i-\frac{1}{2}}^n (q_i^n - q_{i-1}^n) \right) \right] + \left[ \alpha_{i-\frac{1}{2}}^n + \frac{\Delta t}{2} \partial_t \alpha_{i-\frac{1}{2}} \right] \left[ \frac{2+r}{2} (q_{i-1}^n - q_i^n) \right. \\ & \left. - \frac{c}{4} (q_i^n - q_{i-2}^n - q_{i+1}^n + q_{i-1}^n) + \frac{\Delta t}{2\Delta x^2} \left[ 2\alpha_{i-\frac{1}{2}}^n (q_i^n - q_{i-1}^n) \right. \right. \\ & \left. \left. - \alpha_{i-\frac{3}{2}}^n (q_{i-1}^n - q_{i-2}^n) - \alpha_{i+\frac{1}{2}}^n (q_{i+1}^n - q_i^n) \right] \right] \right\} \\ & + r \left[ q_i^n + \left( -\frac{c}{4} (q_{i+1}^n - q_{i-1}^n) + \frac{\Delta t}{2\Delta x^2} \left[ \alpha_{i+\frac{1}{2}}^n (q_{i+1}^n - q_i^n) \right. \right. \right. \\ & \left. \left. - \alpha_{i-\frac{1}{2}}^n (q_i^n - q_{i-1}^n) \right] + \frac{r}{2} q_i^n \right). \end{aligned} \quad (19)$$

where  $c = \frac{\lambda \Delta t}{\Delta x}$  denotes the Courant number and  $r = \beta \Delta t$  is called the reaction number.

**Remark 3** (Constant diffusion coefficient). *If we consider a constant diffusion coefficient and denote  $\alpha \Delta_i^{(2)} = (\Delta \alpha \Delta)_i$ , scheme (18) reads*

$$q_i^{n+1} = q_i^n - \frac{\lambda \Delta t}{\Delta x} \left\{ q_i^n + \frac{1}{2} \Delta x \Delta_i + \frac{\Delta t}{2} \left[ -\lambda \Delta_i + \beta \left( q_i^n + \frac{1}{2} \Delta x \Delta_i \right) + \alpha \Delta_i^{(2)} \right] \right\}$$

$$\begin{aligned}
& -q_{i-1}^n + \frac{1}{2}\Delta x\Delta_{i-1} - \frac{\Delta t}{2} \left[ -\lambda\Delta_{i-1} + \beta \left( q_{i-1}^n - \frac{1}{2}\Delta x\Delta_{i-1} \right) + \alpha\Delta_{i-1}^{(2)} \right] \Big\} \\
& + \frac{\alpha\Delta t}{\Delta x^2} \left\{ (q_{i+1}^n - 2q_i^n + q_{i-1}^n) + \frac{\Delta t}{2} [-\lambda(\Delta_{i+1} - 2\Delta_i + \Delta_{i-1}) \right. \\
& \left. + \alpha(\Delta_{i+1}^{(2)} - 2\Delta_i^{(2)} + \Delta_{i-1}^{(2)}) + \beta(q_{i+1}^n - 2q_i^n + q_{i-1}^n)] \right\} \\
& + \beta\Delta t \left[ q_i^n + \frac{\Delta t}{2} (-\lambda\Delta_i + \alpha\Delta_i^{(2)} + \beta q_i^n) \right]. \tag{20}
\end{aligned}$$

Hence, the scheme for the advection-diffusion-reaction equation with constant diffusion coefficient becomes

$$\begin{aligned}
q_i^{n+1} = & q_i^n - c \left\{ \frac{2+r}{2} (q_i^n - q_{i-1}^n) + \frac{2-2c+r}{8} (q_{i+1}^n - q_{i-1}^n - q_i^n + q_{i-2}^n) \right. \\
& \left. + \frac{d}{2} [q_{i+1}^n - 3q_i^n + 3q_{i-1}^n - q_{i-2}^n] \right\} \\
& + d \left\{ q_{i+1}^n - 2q_i^n + q_{i-1}^n - \frac{c}{4} (q_{i+2}^n - 2q_{i+1}^n + 2q_{i-1}^n - q_{i-2}^n) \right. \\
& \left. + \frac{d}{2} [q_{i+2}^n - 4q_{i+1}^n + 6q_i^n - 4q_{i-1}^n + q_{i-2}^n] + \frac{r}{2} (q_{i+1}^n - 2q_i^n + q_{i-1}^n) \right\} \\
& + r \left[ q_i^n - \frac{c}{4} (q_{i+1}^n - q_{i-1}^n) + \frac{d}{2} [q_{i+1}^n - 2q_i^n + q_{i-1}^n] + \frac{r}{2} q_i^n \right]. \tag{21}
\end{aligned}$$

where  $d = \frac{\alpha\Delta t}{\Delta x^2}$ .

**Remark 4** (Advection-reaction equation). Assuming zero diffusivity, the scheme for the linear advection-reaction equation is recovered from (18),

$$\begin{aligned}
q_i^{n+1} = & q_i^n - \frac{\lambda\Delta t}{\Delta x} \left\{ q_i^n + \frac{1}{2}\Delta x\Delta_i + \frac{\Delta t}{2} [-\lambda\Delta_i + \beta \left( q_i^n + \frac{1}{2}\Delta x\Delta_i \right)] \right. \\
& \left. - q_{i-1}^n + \frac{1}{2}\Delta x\Delta_{i-1} - \frac{\Delta t}{2} [-\lambda\Delta_{i-1} + \beta \left( q_{i-1}^n - \frac{1}{2}\Delta x\Delta_{i-1} \right)] \right\} \\
& + \beta\Delta t \left[ q_i^n + \frac{\Delta t}{2} (-\lambda\Delta_i + \beta q_i^n) \right]. \tag{22}
\end{aligned}$$

Furthermore, using centred slopes we get

$$\begin{aligned}
q_i^{n+1} = & q_i^n - c \left[ \frac{2+r}{2} (q_i^n - q_{i-1}^n) + \frac{2-2c+r}{8} (q_{i+1}^n - q_i^n - q_{i-1}^n + q_{i-2}^n) \right] \\
& + r \left[ q_i^n - \frac{c}{4} (q_{i+1}^n - q_{i-1}^n) + \frac{r}{2} q_i^n \right]. \tag{23}
\end{aligned}$$

**Theorem 5.** Schemes (19), (21) and (23) are second order in space and time.

*Proof.* The detailed proof is included in A. □

**Remark 6.** In case the reconstruction done in Step 1 is done with constant polynomials and the half in time evolution of the variables given by the Taylor series expansion is neglected, the resulting scheme reduces to

$$q_i^{n+1} = q_i^n - c (q_i^n - q_{i-1}^n) - \frac{\Delta t}{\Delta x^2} \left[ \alpha_{i+\frac{1}{2}}^n (q_{i+1}^n - q_i^n) + \alpha_{i-\frac{1}{2}}^n (q_{i-1}^n - q_i^n) \right] + r q_i^n. \tag{24}$$

which is a first order in time and space scheme for the advection-diffusion-reaction equation (1).

## 4 MUSCL-Hancock

The MUSCL-Hancock method, originally credited to Hancock in [47], is extended here to account for the source and diffusion terms. The extension is motivated by the ADER framework introduced earlier. First recall that the MUSCL-Hancock method for the homogeneous linear advection equation has the following steps:

**Step 1.** Data reconstruction. First-degree polynomial for a cell  $i$  are used, namely

$$p_i(x) = q_i^n + \Delta_i(x - x_i).$$

**Step 2.** Computation of boundary extrapolated values. Cell boundary values are computed by simply evaluating the polynomials appropriately

$$q_i^L = p_i(x_{i-\frac{1}{2}}) = q_i^n - \frac{1}{2}\Delta x \Delta_i,$$

$$q_i^R = p_i(x_{i+\frac{1}{2}}) = q_i^n + \frac{1}{2}\Delta x \Delta_i.$$

**Step 3.** Evolution of boundary extrapolated values. Boundary-extrapolated values are evolved by half a time step,

$$\begin{aligned} \bar{q}_i^R &= q_i^R - \frac{\Delta t}{2\Delta x} (f(q_i^R) - f(q_i^L)), \\ \bar{q}_i^L &= q_i^L - \frac{\Delta t}{2\Delta x} (f(q_i^R) - f(q_i^L)). \end{aligned}$$

**Step 4.** Solution of the Riemann problem and numerical flux. The evolved boundary-extrapolated values are used to define a classical Riemann problem at each intercell boundary,

$$\begin{cases} \partial_t q(x, t) + \lambda \partial_x q(x, t) = 0, \\ q(x, 0) = \begin{cases} \bar{q}_i^R & x < 0, \\ \bar{q}_{i+1}^L & x > 0, \end{cases} \end{cases}$$

the solution of which is

$$q(x, t) = \begin{cases} \bar{q}_i^R & \frac{x}{t} < \lambda, \\ \bar{q}_{i+1}^L & \frac{x}{t} > \lambda. \end{cases}$$

Hence, the sought intercell flux is given by

$$f_{i+\frac{1}{2}}^{MH} = \begin{cases} \lambda \bar{q}_i^R = \lambda (q_i^n + \frac{1-c}{2}\Delta x \Delta_i) & \lambda > 0, \\ \lambda \bar{q}_{i+1}^L = \lambda (q_{i+1}^n - \frac{1+c}{2}\Delta x \Delta_{i+1}) & \lambda < 0. \end{cases}$$

Note that if no reconstruction is performed, the MUSCL-Hancock method reduces to the Godunov first-order method, with the particular numerical flux employed in the last step.

By choosing centred slopes, as already done for ADER, and assuming  $\lambda > 0$  (the discussion of the case  $\lambda < 0$  is analogous) we obtain the MUSCL-Hancock scheme for the linear advection equation:

$$q_j^{n+1} = q_j^n - c \left[ q_j^n - q_{j-1}^n + \frac{1-c}{4} (q_{j+1}^n - q_j^n - q_{j-1}^n + q_{j-2}^n) \right]. \quad (25)$$

## 4.1 Source and diffusion terms

The inclusion of reaction and diffusion terms is accomplished by modifying Step 3, in which such terms at the half time are added to the evolution of boundary extrapolated values. Thus we obtain:

$$\begin{aligned} \bar{q}_i^R &= q_i^R - \frac{\Delta t}{2} \left\{ \frac{1}{\Delta x} (f(q_i^R) - f(q_i^L)) \right. \\ &\quad \left. - \frac{1}{\Delta x^2} g((\alpha \Delta q)_i^R, (\alpha \Delta q)_i^L) - s(q_i^R) \right\} \end{aligned} \quad (26)$$

$$\begin{aligned} \bar{q}_i^L &= q_{i+1}^L - \frac{\Delta t}{2} \left\{ \frac{1}{\Delta x} (f(q_{i+1}^R) - f(q_{i+1}^L)) \right. \\ &\quad \left. - \frac{1}{\Delta x^2} g((\alpha \Delta q)_{i+1}^R, (\alpha \Delta q)_{i+1}^L) - s(q_{i+1}^L) \right\} \end{aligned} \quad (27)$$

with

$$g((\alpha \Delta q)_i^R, (\alpha \Delta q)_i^L) = \alpha_{i+\frac{1}{2}}^n (q_{i+1}^n - q_i^n) - \alpha_{i-\frac{1}{2}}^n (q_i^n - q_{i-1}^n).$$

The final step is as before, that is, the numerical flux is computed by solving the Riemann problem for the linear advection equation with evolved boundary-extrapolated values as initial conditions. Just as ADER, the numerical flux includes the contribution due to diffusion and source terms. Additional contributions to the scheme resulting from diffusion and reaction are accounted for by following the ADER approach introduced in Section 3.

**Remark 7.** *The resulting schemes for the linear advection-diffusion-reaction equation, constructed from the ADER and MUSCL-Hancock approaches, are algebraically identical.*

## 5 Stability analysis

The stability analysis of the obtained schemes is divided into two cases. On the one hand, linear advection equation allows for an easy computation of the stability region. On the other hand, advection-diffusion-reaction equation with constant diffusion coefficient will be analysed thanks to graphical representation.

### 5.1 Linear advection equation

Stability analysis of linear models is done following von Neumann stability analysis procedure, see [48], [30]. Let us consider the trial function

$$q_i^n = A^n e^{I\theta i},$$

where  $A \in \mathbb{C}$  represents an amplitude,  $I$  denotes the complex unity so that  $i$  is kept for the mesh, and  $\theta = P\Delta x$  is an angle with  $P$  the wave number in the  $x$ -direction. Then, (25) yields to

$$\begin{aligned} A^{n+1} e^{I\theta i} &= A^n e^{I\theta i} - c \left[ A^n e^{I\theta i} - A^n e^{I\theta(i-1)} + \frac{1-c}{4} (A^n e^{I\theta(i-1)} \right. \\ &\quad \left. - A^n e^{I\theta i} - A^n e^{I\theta(i-1)} + A^n e^{I\theta(i-2)}) \right], \end{aligned}$$

$$A = 1 - c \left[ 1 - e^{-I\theta} + \frac{1-c}{4} (e^{-I\theta} - 1 - e^{-I\theta} + e^{-2I\theta}) \right],$$

hence,

$$\|A\|^2 = c(c-1)(\cos\theta - 1)^2 \left[ \frac{1}{2}c(c-1)(\cos\theta + 1) + 1 \right] + 1.$$

The stability condition,  $\|A\|^2 \leq 1$ , is verified if and only if

$$c(c-1)(\cos\theta - 1)^2 \left[ \frac{1}{2}c(c-1)(\cos\theta + 1) + 1 \right] \leq 0$$

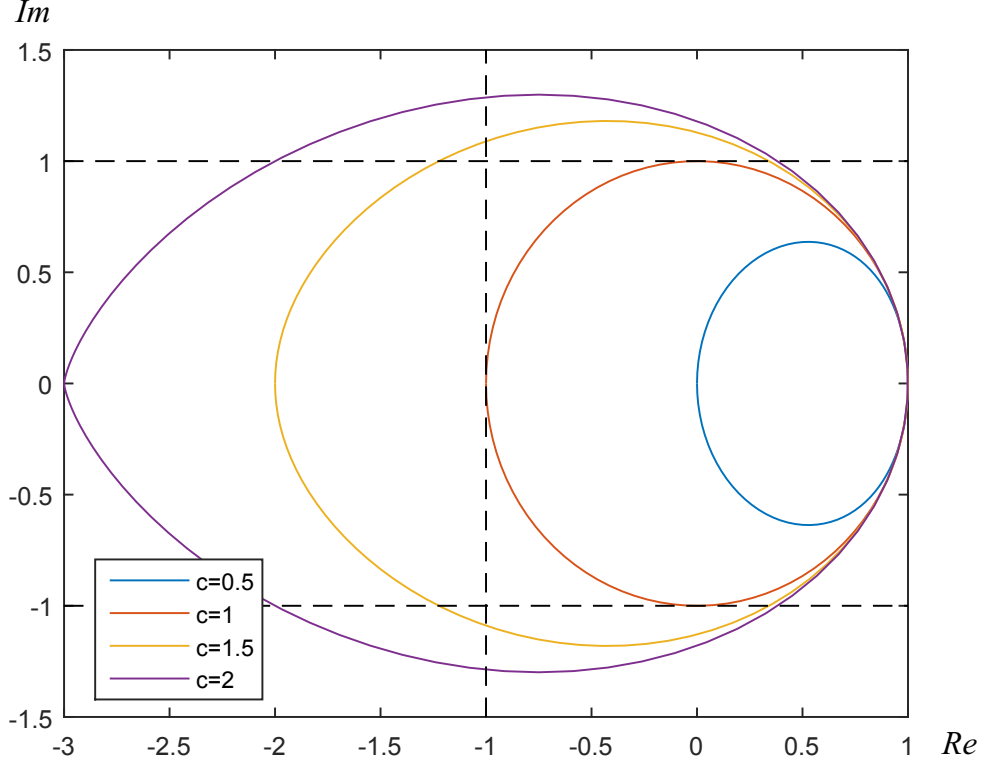


Figure 1: Representation in the complex plane of the amplification factor values for several values of  $c$  with  $\theta \in [-\pi, \pi]$ . It can be observed that  $c$  is bounded above by 1 when  $\|A\|$  is bounded by 1.

$$\Leftrightarrow c(c-1)(\cos\theta+1) \geq -2 \text{ and } c \leq 1.$$

From which it follows that the scheme is stable if the Courant number,  $c$  lies between zero and unity; it is conditionally stable with stability condition

$$0 \leq c \leq 1.$$

Sometimes the amplification factor is a difficult expression to deal with. In order to make it easier, we can represent the value of the function of the binomial expression of the amplification factor,

$$A : [-\pi, \pi] \times \mathbb{R} \longrightarrow \mathbb{C} \\ (\theta, c) \rightsquigarrow A(\theta, c), \quad (28)$$

for different values of  $c$ , see [19]. In Figure 1, we can observe that the functions whose image is completely contained in the square  $[-1, 1] \times [-1, 1] \subset \mathbb{C}$  are defined for  $c \in [0, 1]$ . This agrees with the analytical results already obtained.

On the other hand, we can plot the function defined by the norm of the amplification factor,  $\|A(\theta, c)\|^2 \in \mathbb{R}$ . As  $A$  depends on two variables,  $\theta$  and  $c$ , the plot, Figure 2a, is a surface in  $\mathbb{R}^3$ . Drawing the contour lines we can confirm that the stability condition is verified if and only if  $0 \leq c \leq 1$ . In Figure 2b we consider  $c \in [0, 1.2]$  to remark that for any chosen  $c_0 > 1$  there exist  $\theta_{c_0} \in [-\pi, \pi]$  such that the values of  $\|A(\theta_{c_0}, c_0)\|$  are larger than one.

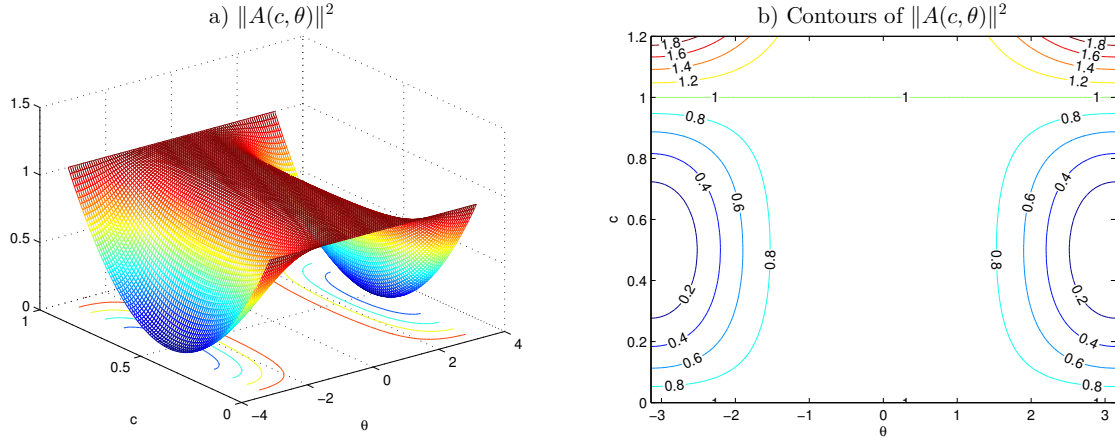


Figure 2: Graph and contour lines of  $\|A(\theta, c)\|^2$  for scheme (25). The stability region is clearly determined for  $0 \leq c \leq 1$ .

## 5.2 Linear advection-diffusion-reaction equation

The amplification factor of scheme (20), which depends on the angle  $\theta$  and on the parameters  $c = \frac{\lambda \Delta t}{\Delta x}$ ,  $d = \frac{\alpha \Delta t}{\Delta x^2}$  and  $r = \beta \Delta t$ , is computed using the von Neumann procedure obtaining

$$\begin{aligned}
A = & 1 - c \left\{ 1 - \cos \theta + I \sin \theta + \frac{1-c}{4} (2I \sin \theta - 1 + \cos(2\theta) - I \sin(2\theta)) \right. \\
& + \frac{r}{2} \left[ 1 - \cos \theta + I \sin \theta + \frac{1}{4} (2I \sin \theta - 1 + \cos(2\theta) - I \sin(2\theta)) \right] \\
& \left. + \frac{d}{2} (4 \cos \theta - 2I \sin \theta - 3 - \cos(2\theta) - I \sin(2\theta)) \right\} \\
& + d \left\{ 2 \cos \theta - 2 - \frac{c}{4} (2I \sin(2\theta) - 6I \sin \theta) + \frac{d}{2} (2 \cos(2\theta) - 8 \cos \theta + 6) \right. \\
& \left. + \frac{r}{2} (2 \cos \theta - 2) \right\} + r \left\{ 1 - \frac{c}{2} I \sin \theta + d (\cos \theta - 1) + \frac{r}{2} \right\}.
\end{aligned}$$

As the bounds of  $c$ ,  $d$  and  $r$  in order to limit the amplification factor are interdependent, the computation of the constraints will produce complicated expressions. Still, a graphical representation provides us with a good approach to determine the stability region.

### Linear advection-reaction equation

The function related with the amplification factor of the linear advection-reaction equation results

$$\begin{aligned}
A : [-\pi, \pi] \times \mathbb{R} \times \mathbb{R} & \longrightarrow \mathbb{R} \\
(\theta, c, r) & \longrightarrow A(\theta, c, r).
\end{aligned}$$

Its graph is embedded in  $\mathbb{R}^4$ , therefore, instead of plotting contour lines, we represent the isosurface of level one which splits  $\mathbb{R}^3$  in two domains (see Figure 3). One of them, which contains the point  $(\theta, c, r) = (0, 0, 0)$ , is the stability region of the scheme. Inside the other domain the scheme is unconditionally unstable. Furthermore, the orthogonal planes to the  $r$ -axis, that is, the planes resulting for a fixed value of  $r$ , provide the contour plots of level one for the linear advection-reaction equation related to the set  $r$  (see the two-dimensional subplots of Figure 3 where  $S$  denotes the stability region of the scheme).

For instance, assuming  $r = -1$  the value  $c = 1.1$  guarantees the stability. However, we must carefully analyse these results. For a specific problem, with a given mesh, setting  $r = -1$  does not imply that the

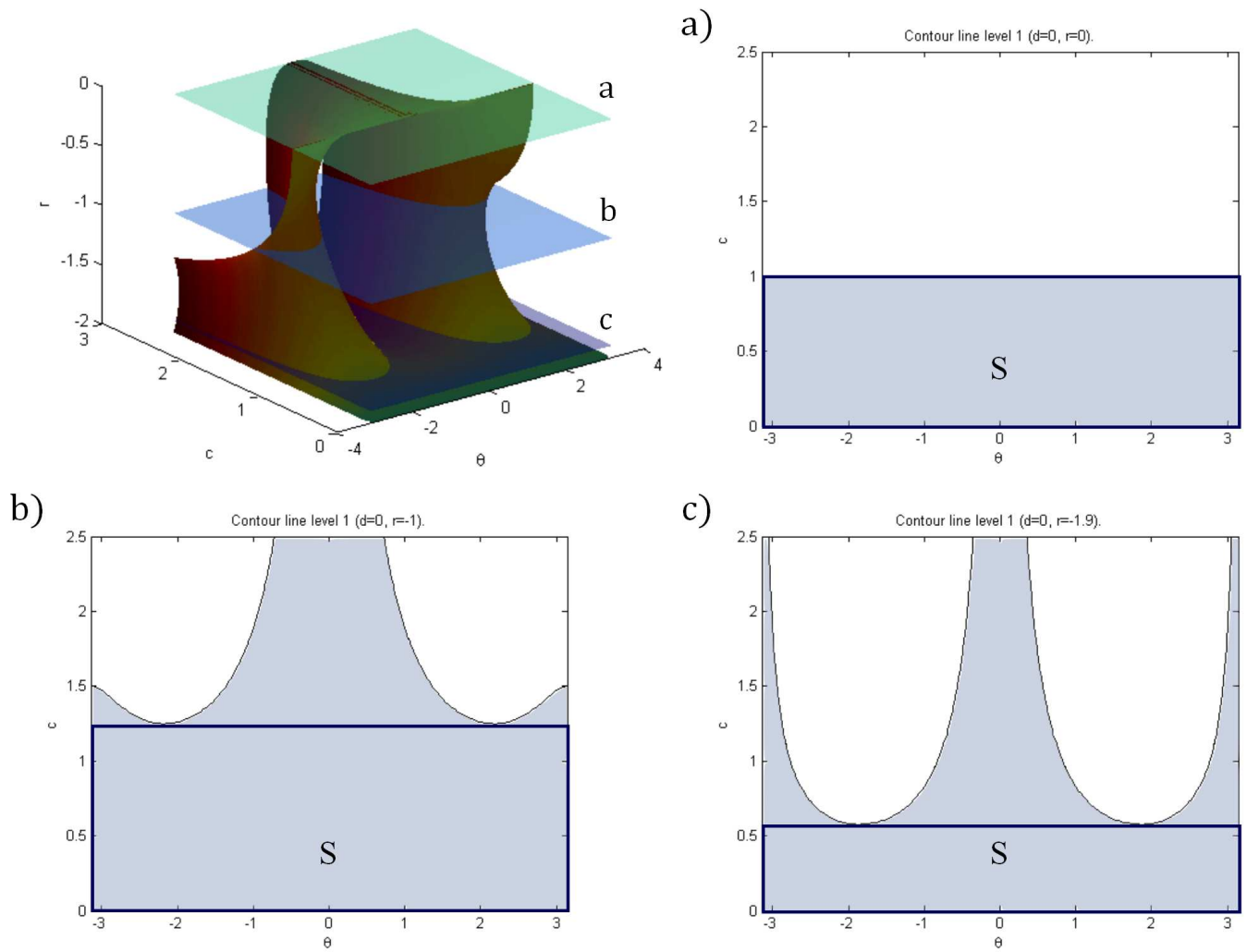


Figure 3: Stability region for the linear advection-reaction equation. The isosurface of level one splits  $\mathbb{R}^3$  into the stability region, containing the origin, and the unstable region. Subplots a), b), c) represent the contour plot of level one for the fixed values of  $r = 0$ ,  $r = -1$  and  $r = -1.9$  respectively. The shaded regions correspond to the stability region. The blue rectangles identified as  $S$  are the admissible regions of stability.

$\Delta t$  is such that  $c = 1.1$  and vice versa. A particular example will help us to understand the situation better. We consider the linear advection-reaction equation

$$\partial_t q(x, t) + \lambda_0 \partial_x q(x, t) = \beta_0 q(x, t)$$

with fixed  $\lambda_0 \in \mathbb{R}^+$ ,  $\beta_0 \in \mathbb{R}^-$ . If the mesh size is  $\Delta x = \Delta x_0$ , then it is verified

$$\begin{cases} r = \beta_0 \Delta t, \\ c = \frac{\lambda_0 \Delta t}{\Delta x_0}. \end{cases} \quad (29)$$

So, if  $\Delta t$  is computed from  $r = r_0$  fixed, then

$$c = \frac{\lambda_0 r_0}{\beta_0 \Delta x_0} \quad (30)$$

is determined. Similarly, given  $c = c_0$  the value of  $\Delta t$  is resolved and

$$r = \frac{\beta_0 c_0 \Delta x_0}{\lambda_0}. \quad (31)$$

Hence, for  $r = -1$  the value of  $c$  is determined and can be different from 1.1. In case it is bigger, we would have fallen into the unstable region.

To avoid the previous trouble, we define rectangular cuboids

$$O_{c,r} = \{(\theta, c, r) \mid \theta \in [-\pi, \pi], c \in [0, c_M], r \in [r_m, 0], c_M \in \mathbb{R}^+, r_m \in \mathbb{R}^-\} \quad (32)$$

embedded in the stability region. Selecting  $c_M = 1$ , the upper bound of  $c$ , and  $r_m = -1$ , the lower bound of  $c$ , the resulting scheme is stable.

### Linear advection-diffusion equation

The previous procedure can also be applied for the linear advection-diffusion equation. Hence, we consider

$$\begin{aligned} A : [-\pi, \pi] \times \mathbb{R} \times \mathbb{R} &\longrightarrow \mathbb{R} \\ (\theta, c, d) &\longrightarrow A(\theta, c, d) \end{aligned}$$

and

$$O_{c,d} = \{(\theta, c, d) \mid \theta \in [-\pi, \pi], c \in [0, c_M], d \in [0, d_M], c_M, d_M \in \mathbb{R}^+\}. \quad (33)$$

In Figure 4, we can observe that  $c_M = 1$  and  $d_M = 0.5$  generate an admissible cuboid.

### Linear advection-diffusion-reaction equation

As the last step, we study the stability for the linear advection-diffusion-reaction equation. The amplification factor function reads

$$\begin{aligned} A : [-\pi, \pi] \times \mathbb{R} \times \mathbb{R} \times \mathbb{R} &\longrightarrow \mathbb{R} \\ (\theta, c, d, r) &\longrightarrow A(\theta, c, d, r). \end{aligned}$$

so its graph belongs to  $\mathbb{R}^5$  and the isosurfaces are embedded in  $\mathbb{R}^4$ . Admissible regions can be established through 4-orthotopes,

$$O_{c,d,r} = \{(\theta, c, r, d) \mid \theta \in [-\pi, \pi], c \in [0, c_M], d \in [0, d_M], r \in [r_m, 0], \quad (34)$$

$$c_M, d_M \in \mathbb{R}^+, r_m \in \mathbb{R}^-\}. \quad (35)$$

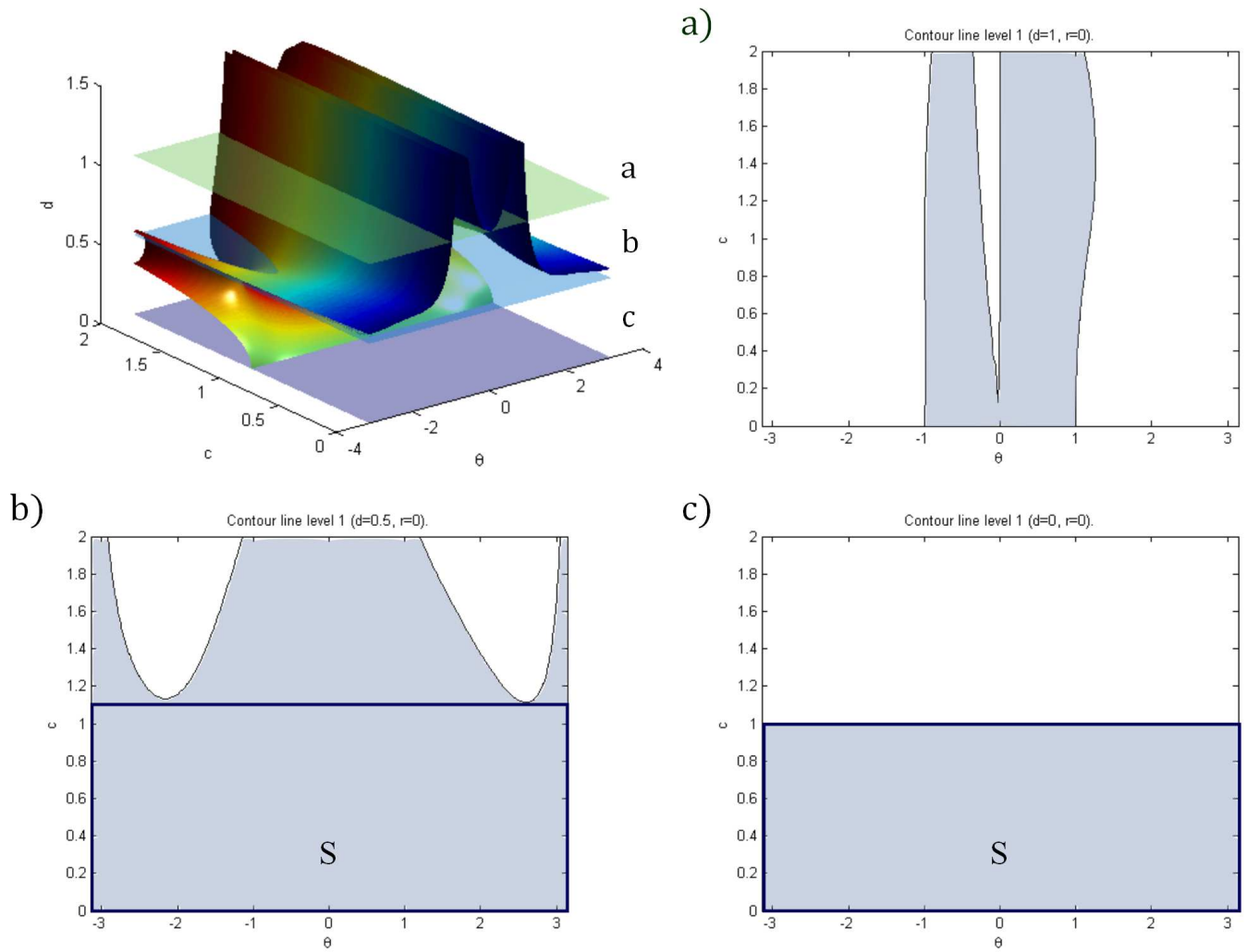


Figure 4: Stability region for the linear advection-diffusion equation. The isosurface of level one splits  $\mathbb{R}^3$  into the stability region, containing the origin, and the unstable region. Subplots a), b), c) represent the contour plot of level one for the fixed values of  $d = 1$ ,  $d = 0.5$  and  $d = 0$  respectively. The shaded regions correspond to the stability region. The blue rectangles identified as  $S$  are the admissible regions of stability.

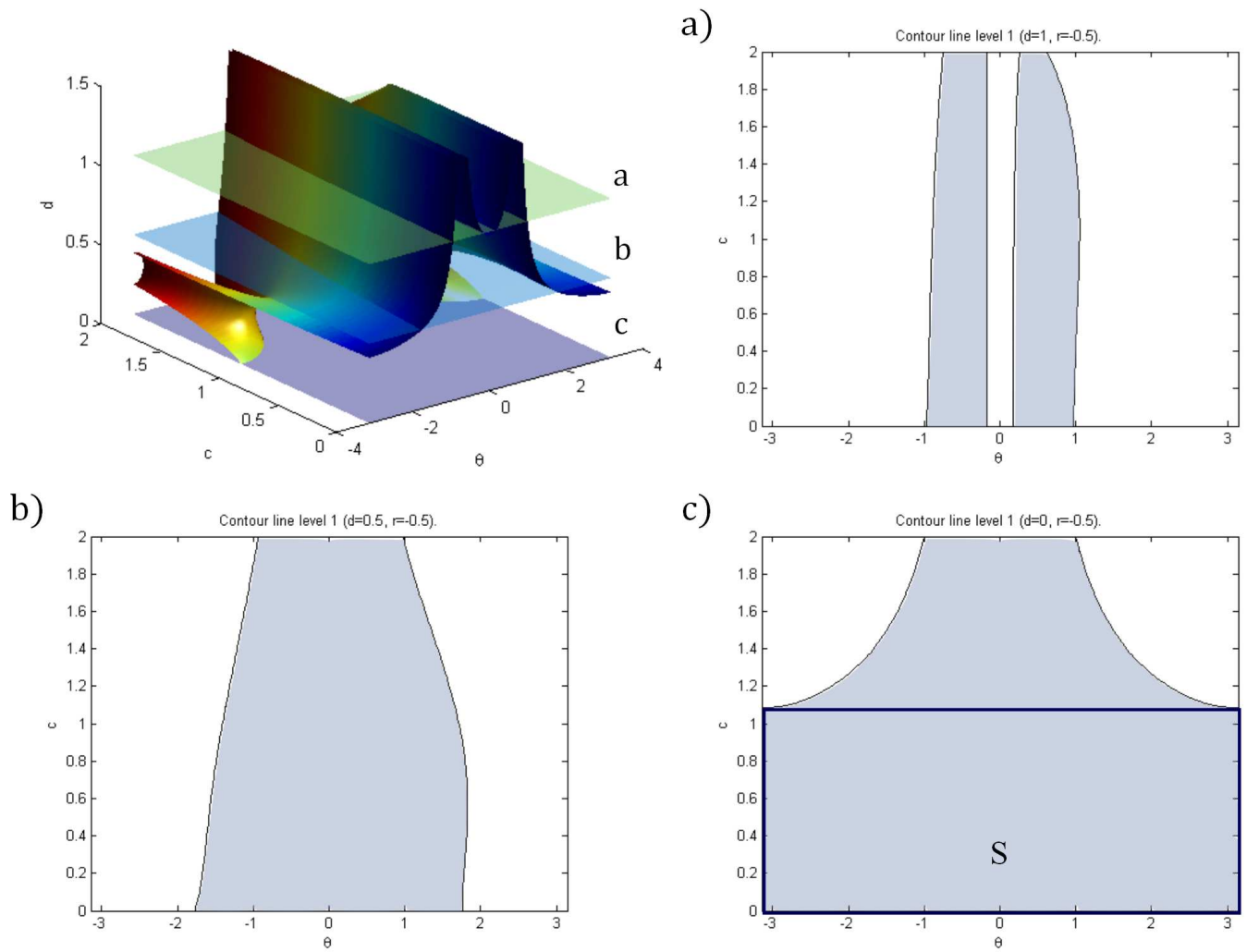


Figure 5: Stability region for the linear advection-diffusion-reaction equation with fixed reaction number  $r = -0.5$ . The isosurface of level one splits  $\mathbb{R}^3$  into the stability region, containing the origin, and the unstable region. Subplots a), b), c) represent the contour plot of level one for the fixed values of  $d = 1$ ,  $d = 0.5$  and  $d = 0$  respectively. The shaded regions correspond to the stability region. The blue rectangles identified as  $S$  are the admissible regions of stability.

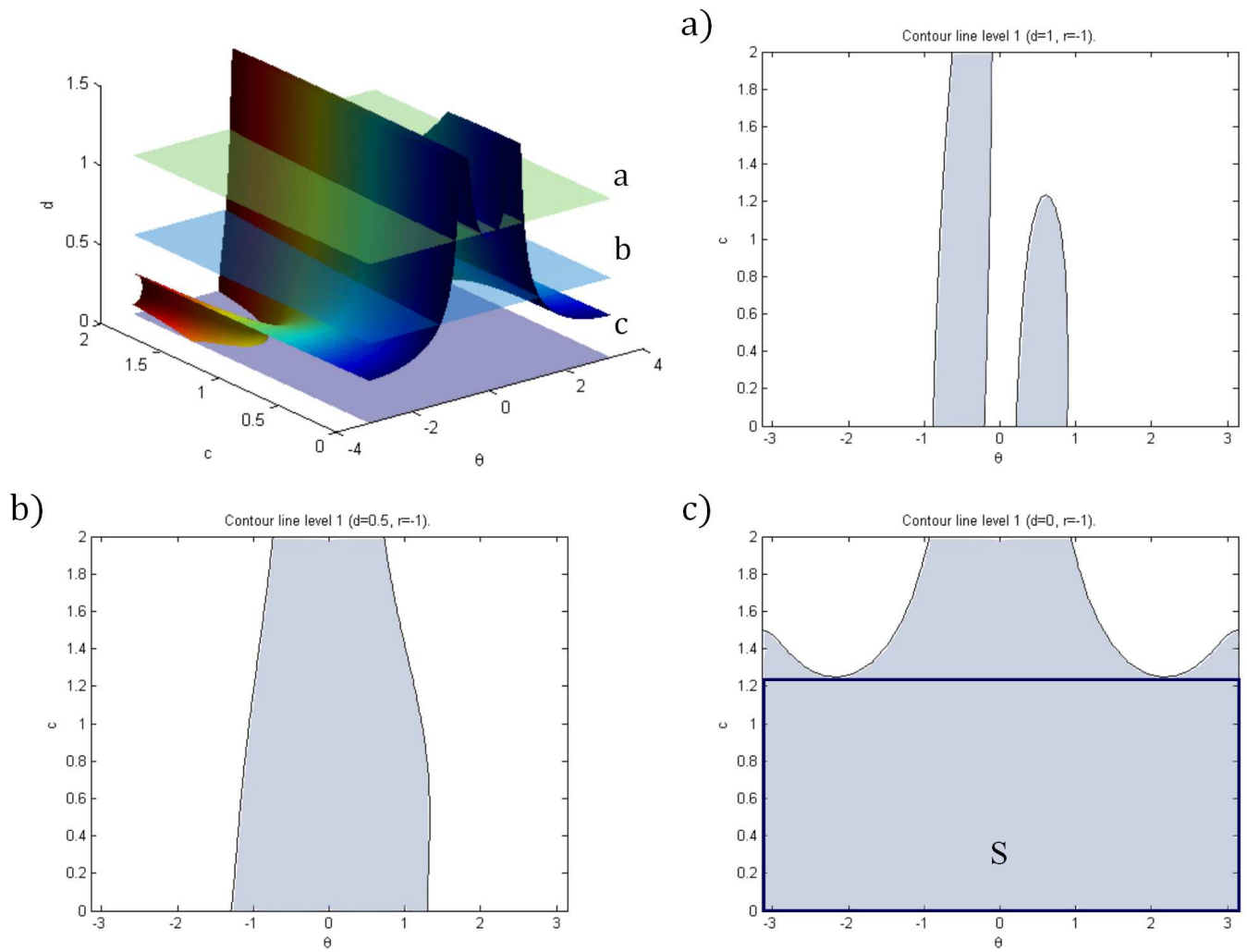


Figure 6: Stability region for the linear advection-diffusion-reaction equation with fixed reaction number  $r = -1$ . The isosurface of level one splits  $\mathbb{R}^3$  into the stability region, containing the origin, and the unstable region. Subplots a), b), c) represent the contour plot of level one for the fixed values of  $d = 1$ ,  $d = 0.5$  and  $d = 0$  respectively. The shaded regions correspond to the stability region. The blue rectangles identified as  $S$  are the admissible regions of stability.

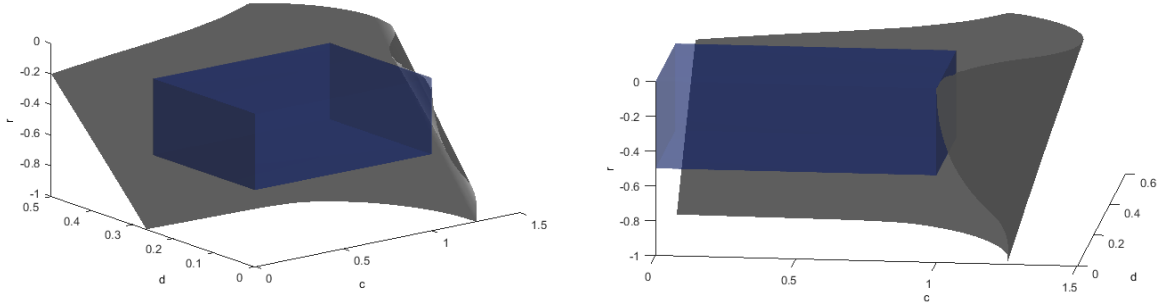


Figure 7: Two different views of the isosurface of level one of function  $m_\theta$ , (36), (grey) and the 4-orthotope of stability  $\mathcal{O}_{1, \frac{1}{4}, -\frac{1}{2}}$  for the linear advection-diffusion-reaction equation (blue).

To get an idea of the shape of the stability region, we can picture an evolutionary problem where one of the variables, for instance  $r$ , plays the role of the time and the remaining ones are considered as spatial variables. Therefore, the stability region is determined by the intersection of the stability regions for the different snapshots of  $r$ . Figures 4-6 show the graphs obtained for fixed values of  $r$ . We can conclude that  $c_M = 1$ ,  $d_M = \frac{1}{4}$  and  $r_m = -\frac{1}{2}$  define a 4-orthotope embedded in the stability region.

A new alternative way to depict the stability region is to plot the isosurface of level one of the function defined by

$$m_\theta(c, d, r) = \max_{\theta \in [-\pi, \pi]} \|A(\theta, c, d, r)\|. \quad (36)$$

Figure 7 confirms that the 4-orthotope defined above,  $\mathcal{O}_{1, \frac{1}{4}, -\frac{1}{2}}$ , is embedded in the stability region.

## 6 Numerical results

In this section, we present the results obtained for several test problems. The error is analysed by computing the norms

$$\text{Err}_{\mathcal{L}^1} = \|q - \hat{q}\|_{l^\infty(\mathcal{L}^1(\Omega))}, \text{Err}_{\mathcal{L}^2} = \|q - \hat{q}\|_{l^\infty(\mathcal{L}^2(\Omega))}, \text{Err}_{\mathcal{L}^\infty} = \|q - \hat{q}\|_{l^\infty(\mathcal{L}^\infty(\Omega))},$$

where  $\hat{q}$  denotes the numerical solution and  $q$  is whether the exact solution or a reference solution computed for a refined mesh if the problem does not have an analytical solution.

### 6.1 Test 1. Advection-reaction equation

We consider two different tests for the advection-reaction equation. For both of them, Dirichlet boundary conditions are set. The exact solution is imposed at the boundary nodes and for the computation of the numerical flux at the first node we use a forward approximation of the slope, namely,

$$\Delta_1 = \frac{q_2 - q_1}{\Delta x},$$

an analogous procedure is considered for the last node.

#### 6.1.1 Test 1.1.

The first test problem studied is given by

$$\partial_t q(x, t) + \partial_x q(x, t) = -q(x, t), \quad q(x, 0) = \exp(-2x^2), \quad (37)$$

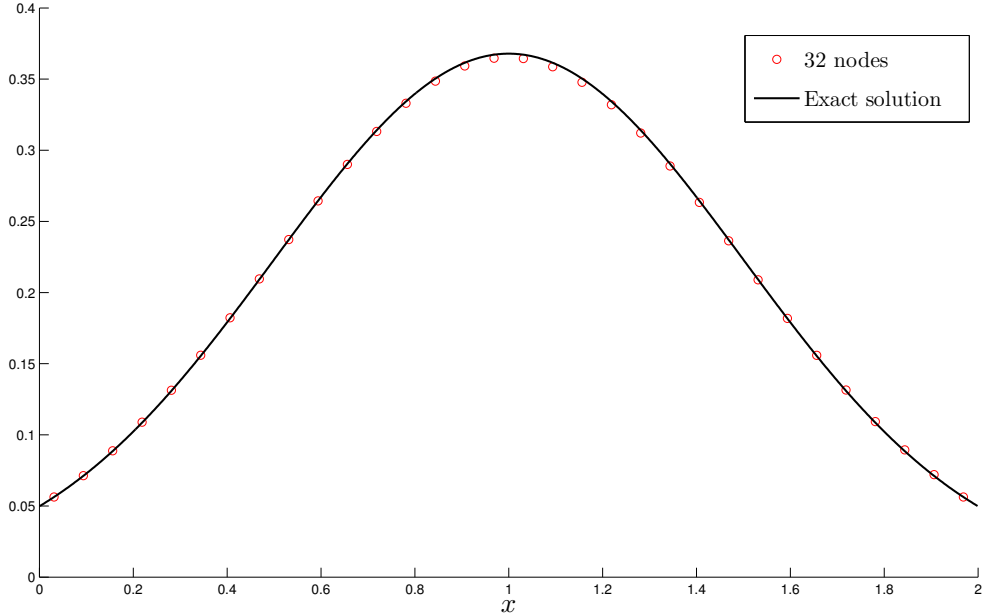


Figure 8: Test 1.1. Exact solution and numerical results obtained for the mesh with 32 nodes.  $\Omega = [0, 2]$ ,  $t_{\text{end}} = 1$ ,  $c = \frac{\lambda \Delta t}{\Delta x} = c_M = 1$ .

with exact solution

$$q(x, t) = \exp(-2(x - \lambda t)^2 + \beta t).$$

Seven meshes are considered. The time step is determined to guarantee that  $c$  and  $r$  belong to the rectangular cuboid (35) defined by  $c_M = 1$ ,  $r_m = -1$ . Since the time step condition imposed by  $c_M$  is lower than the defined by  $r_m$ , the values of  $r$  are computed following (31).

The obtained  $r$ , errors and order are depicted in Table 1. The attained second order was theoretically expected. The results for the mesh with 32 nodes are depicted in Figure 8.

It is important to notice that neither of the chosen values for  $c_M$  and  $r_m$  are the optimal in the case of an advection-reaction equation. That is, within this test the exact solution is not expected to be obtained.

### 6.1.2 Test 1.2.

The second test analysed present a discontinuity in the initial conditions:

$$\begin{aligned} \partial_t q(x, t) + \frac{1}{2} \partial_x q(x, t) &= -q(x, t), \\ q(x, 0) &= \begin{cases} 1 & x \in [\frac{1}{8}, \frac{1}{2}], \\ 0 & x \in [0, \frac{1}{8}) \cup (\frac{1}{2}, \frac{3}{2}]. \end{cases} \end{aligned} \quad (38)$$

Its exact solution reads

$$q(x, t) = \begin{cases} 1 & x - \frac{1}{2}t \in [\frac{1}{8}, \frac{1}{2}], \\ 0 & x - \frac{1}{2}t \in [0, \frac{1}{8}) \cup (\frac{1}{2}, \frac{3}{2}]. \end{cases}$$

In Figure 9 we can observe that the loss of monotonicity of the scheme produces oscillations near the discontinuity. This problem arises from considering centred slopes, (3), which provided a linear scheme.

Cells	Err $_{\mathcal{L}^1}$	$\mathcal{O}_{\mathcal{L}^1}$	Err $_{\mathcal{L}^2}$	$\mathcal{O}_{\mathcal{L}^2}$	Err $_{\mathcal{L}^\infty}$	$\mathcal{O}_{\mathcal{L}^\infty}$	$r$
8	$2.15E-2$		$2.17E-02$		$2.95E-02$		$-\frac{1}{8}$
16	$7.10E-3$	1.6	$6.97E-3$	1.64	$1.03E-2$	1.52	$-\frac{1}{16}$
32	$1.95E-3$	1.87	$1.86E-3$	1.91	$2.77E-3$	1.9	$-\frac{1}{32}$
64	$5.02E-4$	1.96	$4.73E-4$	1.98	$7.00E-4$	1.99	$-\frac{1}{64}$
128	$1.27E-4$	1.99	$1.18E-4$	2.0	$1.74E-4$	2.01	$-\frac{1}{128}$
256	$3.19E-5$	2.0	$2.96E-5$	2.0	$4.33E-5$	2.01	$-\frac{1}{256}$
512	$7.98E-6$	2.0	$7.40E-6$	2.0	$1.08E-5$	2.0	$-\frac{1}{512}$

Table 1: Test 1.1. Columns from second to seventh show the errors and convergence rates obtained. The last column depicts the values obtained for  $r = \beta\Delta t = -\Delta t$ .  $\Omega = [0, 2]$ ,  $t_{\text{end}} = 1$ ,  $c = \frac{\lambda\Delta t}{\Delta x} = c_M = 1$ .

Cells	Err $_{\mathcal{L}^1}$	$\mathcal{O}_{\mathcal{L}^1}$	Err $_{\mathcal{L}^2}$	$\mathcal{O}_{\mathcal{L}^2}$	Err $_{\mathcal{L}^\infty}$	$\mathcal{O}_{\mathcal{L}^\infty}$
8	$2.76E-04$		$4.21E-04$		$7.76E-04$	
16	$1.32E-04$	1.2673	$1.43E-04$	1.5478	$2.07E-04$	1.5336
32	$4.11E-05$	1.7220	$4.01E-05$	1.8914	$6.59E-05$	1.9226
64	$1.25E-05$	1.8921	$1.19E-05$	1.9551	$2.48E-05$	1.9777
128	$3.48E-06$	1.9437	$3.24E-06$	1.9709	$6.92E-06$	1.9850
256	$9.13E-07$	1.9347	$8.39E-07$	1.9501	$1.79E-06$	1.9686
512	$2.67E-07$	1.6799	$2.38E-07$	1.7004	$4.48E-07$	1.7376

Table 2: Test 2.1. Absolute errors and convergence rates obtained.  $\Omega = [-1, 1]$ ,  $t_{\text{end}} = 1$ ,  $c_M = 0.1$ ,  $d_M = 0.25$ ,  $r_m = -0.25$ .

Indeed, we need to circumvent Godunov's theorem to obtain a monotone scheme. This can be done by including non-linear slopes. In the existing literature, the linear advection equation case was already studied combining ADER schemes with ENO, WENO or WAF approaches obtaining good results.

## 6.2 Test 2. Advection-diffusion-reaction equation

Next, we consider two initial value problems for the advection-diffusion-reaction equation.

### 6.2.1 Test 2.1.

Following [41], we set a problem with constant diffusion coefficient:

$$\begin{aligned} \partial_t q(x, t) + 10\partial_x q(x, t) - 10^{-5}\partial_x^{(2)} q(x, t) &= -5q(x, t), \\ q(x, 0) &= \sin(\pi x) \end{aligned}$$

in the computational domain  $\Omega \times T = [-1, 1] \times [0, 1]$  with Dirichlet boundary conditions. The exact solution reads

$$q(x, t) = \exp((-\alpha\pi^2 + \beta)t) \sin(\pi(x - \lambda t)).$$

The numerical results obtained are detailed in Table 2. As the magnitude of the solution is small, relative errors and orders of accuracy are also computed and depicted in Table 3 to facilitate the analysis of the results. The expected second order is attained. The loss of accuracy in infinity norm for the two finer meshes is due to the boundary condition approach.

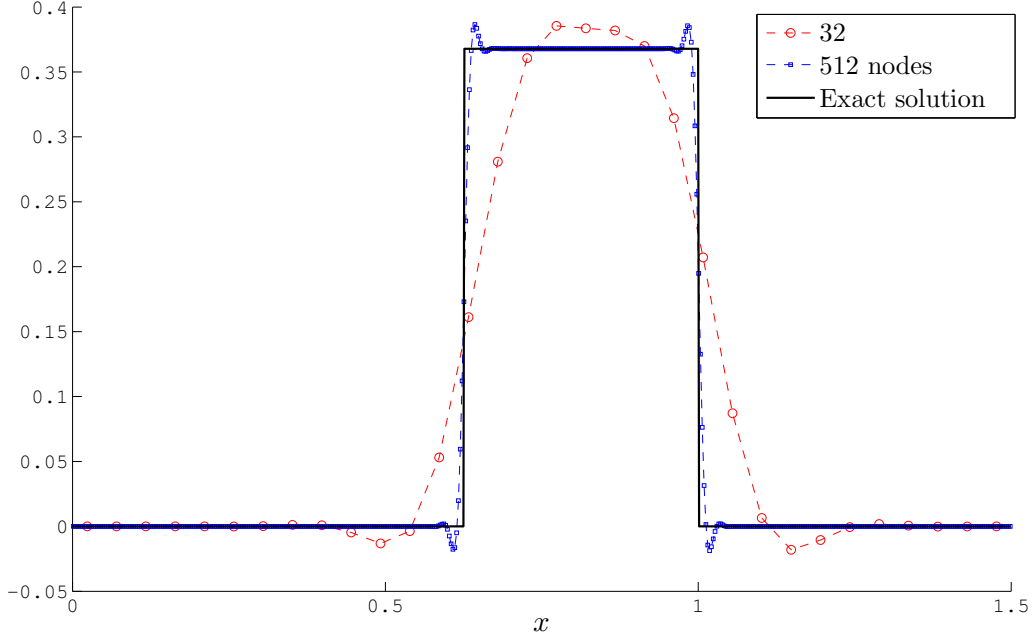


Figure 9: Test 1.2. Exact solution and numerical results obtained for the meshes with 32 and 512 nodes.  $\Omega = [0, 1.5]$ ,  $t_{\text{end}} = 1$ ,  $c_M = 0.5$ ,  $r_m = -1$ .

Cells	$\text{Err}_{\text{rel}\mathcal{L}^1}$	$\mathcal{O}_{\text{rel}\mathcal{L}^1}$	$\text{Err}_{\text{rel}\mathcal{L}^2}$	$\mathcal{O}_{\text{rel}\mathcal{L}^2}$	$\text{Err}_{\text{rel}\mathcal{L}^\infty}$	$\mathcal{O}_{\text{rel}\mathcal{L}^\infty}$
8	$5.1E-03$		$1.0191e-02$		$2.0383e-02$	
16	$1.34E-03$	2.4668	$3.78E-03$	1.9668	$1.07E-02$	1.4668
32	$9.82E-05$	3.2150	$3.93E-04$	2.7150	$1.57E-03$	2.2150
64	$6.22E-06$	3.0442	$3.52E-05$	2.5442	$1.99E-04$	2.0442
128	$5.25E-07$	2.9952	$4.2E-06$	2.4952	$3.36E-05$	1.9952
256	$1.02E-07$	2.9426	$1.16E-06$	2.4426	$1.31E-05$	1.9426
512	$4.05E-08$	2.5185	$6.48E-07$	2.0185	$1.03E-05$	1.5185

Table 3: Test 2.1. Relative errors and convergence rates obtained.  $\Omega = [-1, 1]$ ,  $t_{\text{end}} = 1$ ,  $c_M = 0.1$ ,  $d_M = 0.25$ ,  $r_m = -0.25$ .

Cells	Err $_{\mathcal{L}^1}$	$\mathcal{O}_{\mathcal{L}^1}$	Err $_{\mathcal{L}^2}$	$\mathcal{O}_{\mathcal{L}^2}$	Err $_{\mathcal{L}^\infty}$	$\mathcal{O}_{\mathcal{L}^\infty}$
8	1.39		$7.18E - 1$		$6.90E - 1$	
16	$3.48E - 1$	2.00	$2.00E - 1$	1.84	$2.16E - 1$	1.68
32	$6.98E - 2$	2.32	$4.26E - 2$	2.24	$4.81E - 2$	2.16
64	$1.41E - 2$	2.31	$8.45E - 3$	2.33	$9.55E - 3$	2.33
128	$2.95E - 3$	2.26	$1.73E - 3$	2.29	$1.91E - 3$	2.32
256	$5.51E - 4$	2.42	$3.18E - 4$	2.44	$3.46E - 4$	2.47

Table 4: Test 2.2. Errors and convergence rates obtained.  $\Omega = [0, 2\pi]$ ,  $t_{\text{end}} = 1$ ,  $c_M = 0.5$ ,  $d_M = 0.25$ ,  $r_m = -0.5$ .

Cells	$c$	$d$	$r$
8	0.5	$6.37E - 7$	$-1.96E - 1$
16	0.5	$1.27E - 6$	$-9.82E - 2$
32	0.5	$2.55E - 6$	$-4.92E - 2$
64	0.5	$5.09E - 6$	$-2.45E - 2$
128	0.5	$1.02E - 5$	$-1.23E - 2$
256	0.5	$2.04E - 5$	$-6.14E - 3$

Table 5: Test 2.2. Values of the parameters  $c$ ,  $d$  and  $r$  for the computed time step.  $\Omega = [0, 2\pi]$ ,  $t_{\text{end}} = 1$ ,  $c_M = 0.5$ ,  $d_M = 0.25$ ,  $r_m = -0.5$ .

### 6.2.2 Test 2.2.

We consider the computational domain  $\Omega \times T = [0, 2\pi] \times [0, 1]$  and the initial value problem with a time and space dependent diffusion coefficient given by

$$\begin{aligned} \partial_t q(x, t) + 10\partial_x q(x, t) - 10^{-5}\partial_x [\exp(x(t-1)^2)\partial_x q(x, t)] &= -5q(x, t), \\ q(x, 0) &= \exp(\sin^2(x)), \end{aligned}$$

with periodic boundary conditions. The exact solution for this problem is unknown. Therefore, in order to obtain the error and the order of accuracy, we compare the obtained solutions with a reference solution computed for a finer mesh (512 cells).

The obtained results, confirming second order of accuracy, are depicted in Table 4 and Figure 10.

### 6.3 Test 3. Diffusion equation

As a final example, we consider the non-linear diffusion problem proposed in [39]:

$$\begin{aligned} \partial_t q(x, t) &= \partial_x \left[ (q(x, t))^{-1} \partial_x q(x, t) \right], \\ q(x, 0) &= \frac{\sinh(2)}{\cosh(2) - \sin(\sqrt{2}(x-1))} \end{aligned} \tag{39}$$

with periodic boundary conditions in the computational domain  $\Omega = [-\sqrt{2}\pi, \sqrt{2}\pi]$ . Its exact solution reads

$$q(x, t) = \frac{\sinh(2t+2)}{\cosh(2t+2) - \sin(\sqrt{2}(x-1))}.$$

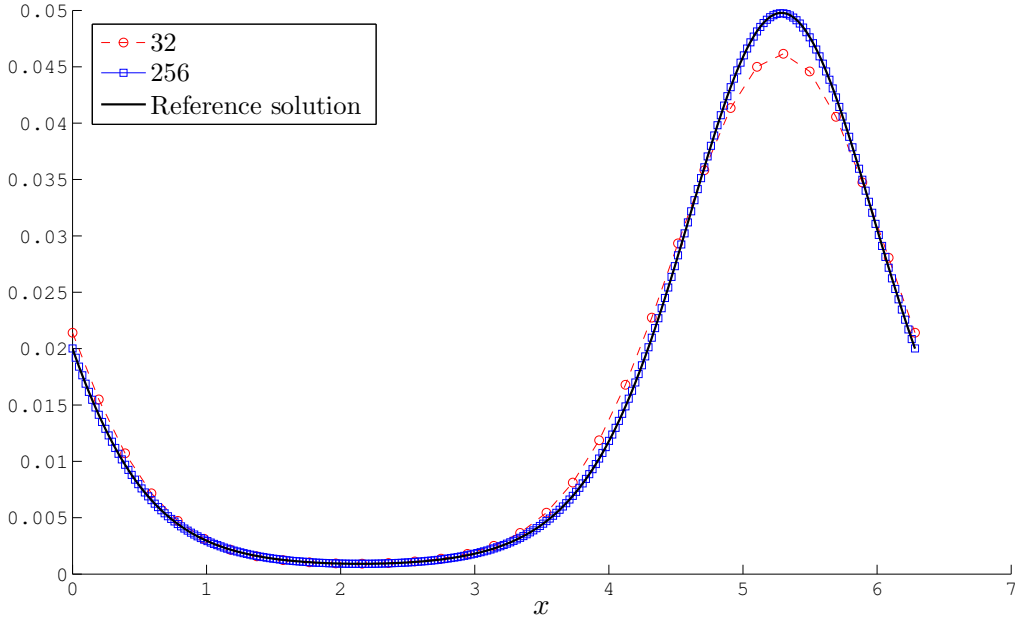


Figure 10: Test 2.2. Exact solution and numerical results obtained for the meshes with 32 and 512 nodes.  $\Omega = [0, 2\pi]$ ,  $t_{\text{end}} = 1$ ,  $c_M = 0.5$ ,  $d_M = 0.25$ ,  $r_m = -0.5$ .

The numerical results presented in Table 6 confirm second order of accuracy. Figure 11 shows the good agreement between the exact solution and the computed solution for two different meshes (32 and 512 nodes).

## 7 Summary and conclusions

In this paper we have constructed numerical schemes of second order of accuracy in both space and time, for solving advection-diffusion-reaction partial differential equations. To this end we have adopted the ADER and the MUSCL-Hancock approaches. Second order of accuracy is ensured by approximating appropriately the integrals that arise in the finite volume framework. For the model equation we have performed a detailed linear stability as well as an accuracy analysis in terms of local truncation error. Empirical convergence rate studies confirm the expected theoretical accuracy analysis. The numeri-

Cells	$\text{Err}_{\mathcal{L}^1}$	$\mathcal{O}_{\mathcal{L}^1}$	$\text{Err}_{\mathcal{L}^2}$	$\mathcal{O}_{\mathcal{L}^2}$	$\text{Err}_{\mathcal{L}^\infty}$	$\mathcal{O}_{\mathcal{L}^\infty}$
8	$1.71E-01$		$6.32E-02$		$3.57E-02$	
16	$3.29E-02$	2.3751	$1.19E-02$	2.4118	$7.56E-03$	2.2391
32	$7.53E-03$	2.1268	$2.79E-03$	2.0897	$1.74E-03$	2.1176
64	$1.83E-03$	2.0413	$6.83E-04$	2.0296	$4.39E-04$	1.989
128	$4.52E-04$	2.0179	$1.70E-04$	2.0103	$1.09E-04$	2.0082
256	$1.12E-04$	2.0075	$4.23E-05$	2.004	$2.73E-05$	1.9993
512	$2.80E-05$	2.0035	$1.06E-05$	2.0017	$6.82E-06$	2.0005

Table 6: Test 3. Errors and convergence rates obtained.  $\Omega = [-\sqrt{2}\pi, \sqrt{2}\pi]$ ,  $t_{\text{end}} = 1$ ,  $d_M = 0.25$ .

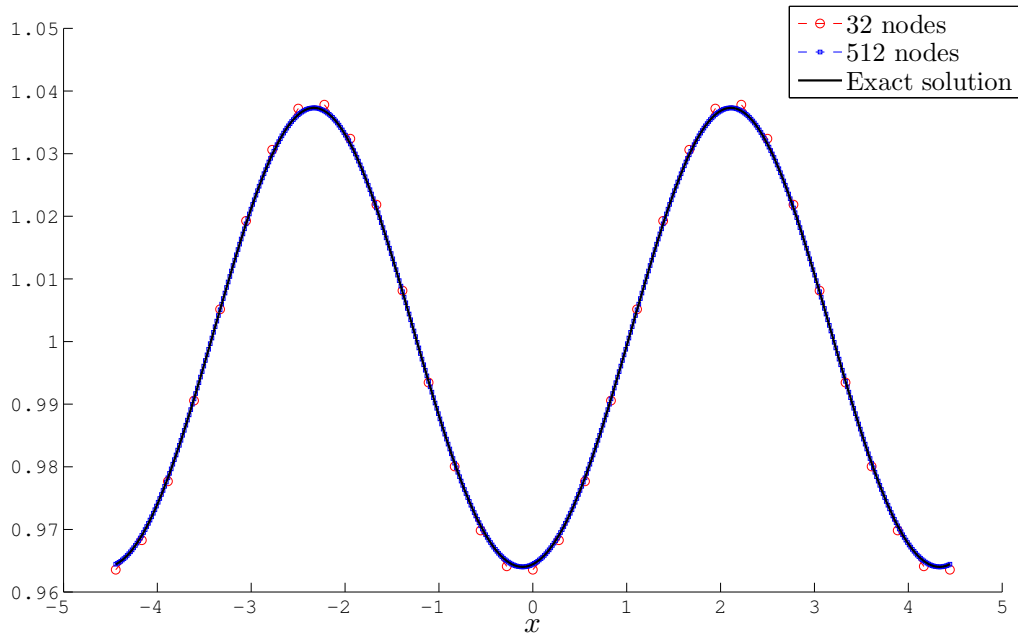


Figure 11: Test 3. Exact solution and numerical results obtained for the meshes with 32 and 512 nodes.  $\Omega = [-\sqrt{2\pi}, \sqrt{2\pi}]$ ,  $t_{\text{end}} = 1$ ,  $d_M = 0.25$ .

cal schemes studied will prove useful in solving systems of time-dependent advection-diffusion-reaction equations for realistic applications.

## Acknowledgements

This work was financially supported by Spanish MICINN projects MTM2008-02483, CGL2011-28499-C03-01 and MTM2013-43745-R; by the Spanish MEC under grant FPU13/00279; by the Xunta de Galicia Consellería de Cultura Educación e Ordenación Universitaria under grant *Axudas de apoio á etapa predoutoral do Plan I2C PRE/2013/031*; by Xunta de Galicia and FEDER under research project GRC2013-014 and by Fundación Barrié under grant *Becas de posgrado en el extranjero 2013*.

## References

- [1] A. Bermúdez, S. Busto, M. Cobas, J. Ferrín, L. Saavedra, and M. E. Vázquez-Cendón. Paths from mathematical problem to technology transfer related with finite volume methods. In *Proceedings of the XXIV Congress on Differential Equations and Applications / XIV Congress on Applied Mathematics*, 2015.
- [2] A. Bermúdez, J.L. Ferrín, L. Saavedra, and M. E. Vázquez-Cendón. A projection hybrid finite volume/element method for low-Mach number flows. *J. Comp. Phys.*, 271:360–378, 2014.
- [3] C. Berthon. Why the MUSCL-Hancock scheme is L1-stable. *Numer. Math.*, 104:27–46, 2006.
- [4] W. Boscheri and M. Dumbser. A direct arbitrary-lagrangian-eulerian ader-weno finite volume scheme on unstructured tetrahedral meshes for conservative and non-conservative hyperbolic systems in 3d. *J. Comput. Phys.*, 275:484–523, 2014.

- [5] A. Canestrelli, A. Siviglia, M. Dumbser, and E. F. Toro. Well-balanced high-order centred schemes for non-conservative hyperbolic systems. Applications to shallow water equations with fixed and mobile bed. *Advances in Water Resources*, 32(6):834–844, 2009.
- [6] C. E. Castro and E. F. Toro. Solvers for the high-order Riemann problem for hyperbolic balance laws. *J. Comp. Phys.*, 227(4):2481–2513, 2008.
- [7] L. Cea and M. E. Vázquez-Cendón. Analysis of a new Kolgan-type scheme motivated by the shallow water equations. *Appl. Num. Math.*, 62(4):489–506, 2012.
- [8] S. Clain and G. J. Machado. A very high-order finite volume method for the time-dependent convection-diffusion problem with Butcher Tableau extension. *Comput. Math. Appl.*, 68(10):1292–1311, 2014.
- [9] S. Clain, G. J. Machado, J. M. Nóbrega, and R. M. S. Pereira. A sixth-order finite volume method for multidomain convection-diffusion problem with discontinuous coefficients. *Comp. Meth. Appl. Mech. Eng.*, 267:43–64, 2013.
- [10] P. Colella. Multidimensional upwind methods for hyperbolic conservation laws. *J. Comput. Phys.*, 87(1):171–200, 1990.
- [11] M. Dumbser. Arbitrary high order PNPM schemes on unstructured meshes for the compressible Navier-Stokes equations. *Comput. Fluids*, 39(1):60–76, 2010.
- [12] M. Dumbser and C. D. Munz. ADER discontinuous Galerkin schemes for aeroacoustics. *CR Acad. Sci. II B*, 333(9):683–687, 2005.
- [13] G. Gassner, F. Lorcher, and C. D. Munz. A contribution to the construction of diffusion fluxes for finite volume and discontinuous Galerkin schemes. *J. Comp. Phys.*, 224(2):1049 – 1063, 2007.
- [14] E. Godlewski and P. A. Raviart. *Numerical Approximation of Hyperbolic Systems of Conservation Laws*, volume 118 of *Applied Mathematical Sciences*. Springer-Verlag New York, 1996.
- [15] S. K. Godunov. A finite difference method for the computation of discontinuous solutions of the equations of fluid dynamics. *Mat. Sb.*, 47:357–393, 1959.
- [16] A. Harten, B. Engquist, S. Osher, and S. R. Chakravarthy. Uniformly high order accurate essentially non-oscillatory schemes, III. In *Upwind and High-Resolution Schemes*, pages 218–290. Springer, 1987.
- [17] J.A. Hernández. High-order finite volume schemes for the advection–diffusion equation. *Int. J. Numer. Meth. Eng.*, 53(5):1211–1234, 2002.
- [18] A. Hidalgo and M. Dumbser. ADER schemes for nonlinear systems of stiff advection–diffusion–reaction equations. *J. Sci. Comput.*, 48(1-3):173–189, 2011.
- [19] K.A. Hoffmann. *Computational fluid dynamics for engineers*. EES, 1989.
- [20] L. Ivan and C.P.T. Groth. High-order solution-adaptive central essentially non-oscillatory (CENO) method for viscous flows. *J. Comput. Phys.*, 257, Part A:830–862, 2014.
- [21] V. P. Kolgan. Application of the principle of minimizing the derivative to the construction of finite-difference schemes for computing discontinuous solutions of gas dynamics. *J. Comput. Phys.*, 230(7):2384–2390, 2011.
- [22] Peter Lax and Burton Wendroff. Systems of conservation laws. *Commun. Pur. Appl. Math.*, 13(2):217–237, 1960.
- [23] Peter D Lax. Hyperbolic systems of conservation laws II. *Commun. Pur. Appl. Math.*, 10(4):537–566, 1957.

- [24] R. J. LeVeque. *Finite Volume Methods for Hyperbolic Problems*. Cambridge Texts in Applied Mathematics. August 2002.
- [25] X. D. Liu, S. Osher, and T. Chan. Weighted essentially non-oscillatory schemes. *J. Comp. Phys.*, 115(1):200–212, 1994.
- [26] G. I. Montecinos and E. F. Toro. Reformulations for general advection–diffusion–reaction equations and locally implicit ADER schemes. *J. Comput. Phys.*, 275:415–442, 2014.
- [27] Javier Murillo and P García-Navarro. Improved riemann solvers for complex transport in two-dimensional unsteady shallow flow. *J. Comput. Phys.*, 230(19):7202–7239, 2011.
- [28] C. Ollivier-Gooch and M. van Altena. A high-order-accurate unstructured mesh finite-volume scheme for the advection-diffusion equation. *J. Comp. Phys.*, 181(2):729–752, 2002.
- [29] C. W. Shu and S. Osher. Efficient implementation of essentially non-oscillatory shock-capturing schemes. *J. Comp. Phys.*, 77(2):439–471, 1988.
- [30] John C Strikwerda. *Finite difference schemes and partial differential equations*. SIAM, 2004.
- [31] Peter K Sweby. High resolution schemes using flux limiters for hyperbolic conservation laws. *SIAM J. Num. Anal.*, 21(5):995–1011, 1984.
- [32] Y. Takakura. Direct-expansion forms of ADER schemes for conservation laws and their verification. *J. Comp. Phys.*, 219(2):855–878, 2006.
- [33] V. A. Titarev. *Derivative Riemann Problem and ADER schemes*. PhD thesis, Università degli studi di Trento, 2005.
- [34] V. A. Titarev and E. F. Toro. ADER schemes for three-dimensional non-linear hyperbolic systems. *J. Comp. Phys.*, 204(2):715–736, 2005.
- [35] V. A. Titarev and E. F. Toro. ADER schemes for hyperbolic conservation laws with reactive terms. In *ECCOMAS CFD 2006: Proceedings of the European Conference on Computational Fluid Dynamics, Egmond aan Zee, The Netherlands, September 5-8, 2006*. Delft University of Technology; European Community on Computational Methods in Applied Sciences (ECCOMAS), 2006.
- [36] V. A. Titarev and E. F. Toro. Analysis of ADER and ADER-WAF schemes. *IMA J Num. Anal.*, 27(3):616–630, 2007.
- [37] E. F. Toro. *Riemann Solvers and Numerical Methods for Fluid Dynamics: A Practical Introduction*. Springer, 3rd Edition, 2009.
- [38] E. F. Toro, M. Dumbser, V. A. Titarev, and M. Käser. The derivative riemann problem: the basis for high order ADER schemes. In *ECCOMAS CFD 2006: Proceedings of the European Conference on Computational Fluid Dynamics, Egmond aan Zee, The Netherlands, September 5-8, 2006*. Delft University of Technology; European Community on Computational Methods in Applied Sciences (ECCOMAS), 2006.
- [39] E. F. Toro and A. Hidalgo. ADER finite volume schemes for nonlinear reaction-diffusion equations. *Appl. Num. Math.*, 59:73–100, 2009.
- [40] E. F. Toro, R. C. Millington, and L. A. M. Nejad. *Godunov Methods*, chapter Towards Very High Order Godunov Schemes. Springer, 2001.
- [41] E. F. Toro and G. I. Montecinos. Advection-diffusion-reaction equations: hyperbolization and high-order ADER discretizations. *SIAM J. Sci. Comp.*, 36(5):A2423–A2457, 2014.
- [42] E. F. Toro and V. A. Titarev. ADER: Towards arbitrary order non-oscillatory schemes for advection-diffusion-reaction. *Proceedings of 8th Taiwan National Conference on Computational Fluid Dynamics*, 2001.

- [43] E. F. Toro and V. A. Titarev. ADER schemes for scalar non-linear hyperbolic conservation laws with source terms in three-space dimensions. *J. Comp. Phys.*, 202(1):196–215, 2005.
- [44] E. F. Toro and V. A. Titarev. TVD fluxes for the high-order ADER schemes. *J. Sci. Comp.*, 24(3):285–309, 2005.
- [45] E. F. Toro and V. A. Titarev. Derivative riemann solvers for systems of conservation laws and ADER methods. *J. Comp. Phys.*, 212(1):150–165, 2006.
- [46] B. van Leer. On the relation between the upwind-differencing schemes of Godunov, Engquist-Osher and Roe. *SIAM J. Sci. Stat. Comp.*, 5(1):1–20, 1984.
- [47] Bram van Leer. Towards the ultimate conservative difference scheme. *J. Comp. Phys.*, 135(2):229–248, 1997.
- [48] M. E. Vázquez-Cendón. *Solving Hyperbolic Equations with Finite Volume Methods*. Springer, 2015.
- [49] H.Y. Zahran. Central ADER schemes for hyperbolic conservation laws. *J. Math. Anal. Appl.*, 346(1):120–140, 2008.

## A Truncation error

In this appendix, the order of accuracy of the attained schemes is analysed. Two distinct cases are studied: the linear advection-reaction equation and the advection-diffusion-reaction equation with time and space dependent diffusion coefficient.

### A.1 Truncation error of the linear advection-reaction equation

Using Taylor series expansion, second order in space and time can be proved for scheme (22) with centred slopes:

$$\begin{aligned}
\tau_j^n &= \frac{1}{\Delta t} [q(x_j, t^{n+1}) - q(x_j, t^n)] + \frac{\lambda}{\Delta x} \left\{ [q(x_j, t^n) - q(x_{j-1}, t^n)] \right. \\
&+ \frac{1}{4} [q(x_{j+1}, t^n) - q(x_j, t^n) - q(x_{j-1}, t^n) + q(x_{j-2}, t^n)] \\
&+ \frac{\Delta t}{2} \left[ -\frac{\lambda}{2\Delta x} [q(x_{j+1}, t^n) - q(x_j, t^n) - q(x_{j-1}, t^n) + q(x_{j-2}, t^n)] \right. \\
&+ \frac{\beta}{\Delta x} \left( [q(x_j, t^n) - q(x_{j-1}, t^n)] \right. \\
&+ \left. \left. \frac{1}{4} [q(x_{j+1}, t^n) - q(x_j, t^n) - q(x_{j-1}, t^n) + q(x_{j-2}, t^n)] \right) \right] \left. \right\} \\
&- \frac{\beta}{\Delta x} \left[ q(x_j, t^n) + \frac{\Delta t}{2} \left( -\frac{\lambda}{2\Delta x} (q(x_{j+1}, t^n) - q(x_{j-1}, t^n)) + \beta q(x_j, t^n) \right) \right] \\
= &\partial_t q(x_j, t^n) + \lambda \partial_x q(x_j, t^n) - \beta q(x_j, t^n) \\
&+ \lambda \left[ -\frac{1}{2} \partial_x^{(2)} q(x_j, t^n) \Delta x + \frac{1}{6} \partial_x^{(3)} q(x_j, t^n) \Delta x^2 \right. \\
&+ \left. \frac{1}{4} \left[ 2\partial_x^{(2)} q(x_j, t^n) \Delta x - \partial_x^{(3)} q(x_j, t^n) \Delta x^2 \right] \right] \\
&+ \Delta t \left\{ \frac{1}{2} \partial_t^{(2)} q(x_j, t^n) + \frac{\lambda}{2} \left[ -\frac{\lambda}{2} \left[ 2\partial_x^{(2)} q(x_j, t^n) - \partial_x^{(3)} q(x_j, t^n) \Delta x \right] \right. \right. \\
&+ \left. \left. \beta \left( \partial_x q(x_j, t^n) - \frac{1}{2} \partial_x^{(2)} q(x_j, t^n) \Delta x + \frac{1}{6} \partial_x^{(3)} q(x_j, t^n) \Delta x^2 \right) \right] \right\}
\end{aligned}$$

$$\begin{aligned}
& + \frac{1}{4} \left[ 2\partial_x^{(2)} q(x_j, t^n) \Delta x - \partial_x^{(3)} q(x_j, t^n) \Delta x^2 \right] \Bigg] \\
& - \frac{\beta}{2} \left[ -\frac{\lambda}{2\Delta x} \left( 2\partial_x q(x_j, t^n) \Delta x + \frac{1}{3} \partial_x^{(3)} q(x_j, t^n) \Delta x^3 \right) + \beta q(x_j, t^n) \right] \Bigg\} \\
& + \mathcal{O}(\Delta t^2) + \mathcal{O}(\Delta x^2) + \mathcal{O}(\Delta x \Delta t) \\
= & \frac{\Delta t}{2} \left[ \partial_t^{(2)} q(x_j, t^n) - \lambda^2 \partial_x^{(2)} q(x_j, t^n) + 2\lambda\beta \partial_x q(x_j, t^n) - \beta^2 q(x_j, t^n) \right] \\
& + \mathcal{O}(\Delta t^2) + \mathcal{O}(\Delta x^2) + \mathcal{O}(\Delta x \Delta t) \\
= & \mathcal{O}(\Delta t^2) + \mathcal{O}(\Delta x^2) + \mathcal{O}(\Delta x \Delta t).
\end{aligned}$$

The last equality arises from

$$\partial_t^{(2)} q(x_j, t^n) - \lambda^2 \partial_x^{(2)} q(x_j, t^n) + \lambda\beta \partial_x q(x_j, t^n) = -\lambda\beta \partial_x q(x_j, t^n) - \beta^2 q(x_j, t^n)$$

which is obtained following the Cauchy-Kovalevskaya procedure.

## A.2 Truncation error of the advection-diffusion-reaction equation

The truncation error of the scheme for the advection-diffusion-reaction equation with time and space dependent diffusion coefficient is given by

$$\begin{aligned}
\tau_j^n = & \frac{1}{\Delta t} [q(x_j, t^{n+1}) - q(x_j, t^n)] + \frac{\lambda}{\Delta x} \left\{ [q(x_j, t^n) - q(x_{j-1}, t^n)] \right. \\
& + \frac{1}{4} [q(x_{j+1}, t^n) - q(x_j, t^n) - q(x_{j-1}, t^n) + q(x_{j-2}, t^n)] \\
& + \frac{\Delta t}{2} \left[ -\frac{\lambda}{2\Delta x} [q(x_{j+1}, t^n) - q(x_j, t^n) - q(x_{j-1}, t^n) + q(x_{j-2}, t^n)] \right. \\
& + \frac{1}{\Delta x} \left[ \left( \alpha(x_{j+\frac{1}{2}}, t^n) \frac{q(x_{j+1}, t^n) - q(x_j, t^n)}{\Delta x} - \alpha(x_{j-\frac{1}{2}}, t^n) \frac{q(x_j, t^n) - q(x_{j-1}, t^n)}{\Delta x} \right) \right. \\
& \left. \left. - \left( \alpha(x_{j-\frac{1}{2}}, t^n) \frac{q(x_j, t^n) - q(x_{j-1}, t^n)}{\Delta x} - \alpha(x_{j-\frac{3}{2}}, t^n) \frac{q(x_{j-1}, t^n) - q(x_{j-2}, t^n)}{\Delta x} \right) \right] \right\} \\
& + \frac{\beta}{\Delta x} \left( [q(x_j, t^n) - q(x_{j-1}, t^n)] + \frac{1}{4} [q(x_{j+1}, t^n) - q(x_j, t^n) \right. \\
& \left. - q(x_{j-1}, t^n) + q(x_{j-2}, t^n)] \right) \Bigg\} - \frac{1}{\Delta x^2} \left\{ \bar{\alpha}(x_{j+\frac{1}{2}}, t^n) [q(x_{j+1}, t^n) - q(x_j, t^n) \right. \\
& + \frac{\Delta t}{2} \left( -\lambda [q(x_{j+2}, t^n) - 2q(x_{j+1}, t^n) + q(x_j, t^n)] + \frac{1}{\Delta x^2} \alpha(x_{j+\frac{3}{2}}, t^n) \right. \\
& [q(x_{j+2}, t^n) - q(x_{j+1}, t^n)] - \frac{1}{\Delta x^2} \alpha(x_{j+\frac{1}{2}}, t^n) [2q(x_{j+1}, t^n) - 2q(x_j, t^n)] \\
& \left. \left. + \frac{1}{\Delta x^2} \alpha(x_{j-\frac{1}{2}}, t^n) [q(x_j, t^n) - q(x_{j-1}, t^n)] + \beta [q(x_{j+1}, t^n) - q(x_j, t^n)] \right) \right] \\
& + \bar{\alpha}(x_{j-\frac{1}{2}}, t^n) \left[ q(x_{j-1}, t^n) - q(x_j, t^n) + \frac{\Delta t}{2} \left( -\lambda [-q(x_{j+1}, t^n) + 2q(x_j, t^n) \right. \right. \\
& \left. \left. - q(x_{j-1}, t^n)] - \frac{1}{\Delta x^2} \alpha(x_{j+\frac{1}{2}}, t^n) [q(x_{j+1}, t^n) - q(x_j, t^n)] \right) \right. \\
& \left. + \frac{1}{\Delta x^2} \alpha(x_{j-\frac{1}{2}}, t^n) [2q(x_j, t^n) - 2q(x_{j-1}, t^n)] - \frac{1}{\Delta x^2} \alpha(x_{j-\frac{3}{2}}, t^n) [q(x_{j-1}, t^n) \right. \\
& \left. \left. - q(x_{j-2}, t^n)] + \beta [q(x_{j-1}, t^n) - q(x_j, t^n)] \right) \right] \Bigg\}
\end{aligned}$$

$$\begin{aligned}
& -\frac{\beta}{\Delta x} \left\{ q(x_j, t^n) + \frac{\Delta t}{2} \left[ -\frac{\lambda}{2\Delta x} [q(x_{j+1}, t^n) - q(x_{j-1}, t^n)] \right. \right. \\
& + \frac{1}{\Delta x^2} \left( \alpha(x_{j+\frac{1}{2}}, t^n) [q(x_{j+1}, t^n) - q(x_j, t^n)] - \alpha(x_{j-\frac{1}{2}}, t^n) [q(x_j, t^n) - q(x_{j-1}, t^n)] \right) \\
& \left. \left. + \frac{\beta}{2\Delta x} q(x_j, t^n) \right] \right\}
\end{aligned}$$

where

$$\bar{\alpha}(x_{j+\frac{1}{2}}, t^n) = \alpha(x_{j+\frac{1}{2}}, t^n) + \frac{\Delta t}{2} \partial_t \alpha(x_{j+\frac{1}{2}}, t^n),$$

$$\bar{\alpha}(x_{j-\frac{1}{2}}, t^n) = \alpha(x_{j-\frac{1}{2}}, t^n) + \frac{\Delta t}{2} \partial_t \alpha(x_{j-\frac{1}{2}}, t^n).$$

Then, we can proceed analysing each of the terms which depend on the diffusion term:

- Local truncation error contribution of the diffusion term to the flux term:

$$\begin{aligned}
& \frac{\lambda \Delta t}{2\Delta x^2} \left\{ \left[ \alpha(x_{j+\frac{1}{2}}, t^n) \frac{q(x_{j+1}, t^n) - q(x_j, t^n)}{\Delta x} - \alpha(x_{j-\frac{1}{2}}, t^n) \frac{q(x_j, t^n) - q(x_{j-1}, t^n)}{\Delta x} \right] \right. \\
& \left. - \left[ \alpha(x_{j-\frac{1}{2}}, t^n) \frac{q(x_j, t^n) - q(x_{j-1}, t^n)}{\Delta x} - \alpha(x_{j-\frac{3}{2}}, t^n) \frac{q(x_{j-1}, t^n) - q(x_{j-2}, t^n)}{\Delta x} \right] \right\} \\
= & \frac{\lambda \Delta t}{2\Delta x^3} \left\{ \left[ \alpha(x_{j+\frac{1}{2}}, t^n) \left( q(x_j, t^n) + \partial_x q(x_j, t^n) \Delta x + \frac{1}{2} \partial^{(2)} q(x_j, t^n) \Delta x^2 \right. \right. \right. \\
& + \frac{1}{6} \partial^{(3)} q(x_j, t^n) \Delta x^3 + \mathcal{O}(\Delta x^4) - q(x_j, t^n) \left. \right) - \alpha(x_{j-\frac{1}{2}}, t^n) \left( q(x_j, t^n) - q(x_j, t^n) \right. \\
& + \partial_x q(x_j, t^n) \Delta x - \frac{1}{2} \partial^{(2)} q(x_j, t^n) \Delta x^2 + \frac{1}{6} \partial^{(3)} q(x_j, t^n) \Delta x^3 + \mathcal{O}(\Delta x^4) \left. \right) \left. \right] \\
& - \left[ \alpha(x_{j-\frac{1}{2}}, t^n) \left( q(x_j, t^n) - q(x_j, t^n) + \partial_x q(x_j, t^n) \Delta x - \frac{1}{2} \partial^{(2)} q(x_j, t^n) \Delta x^2 \right. \right. \\
& + \frac{1}{6} \partial^{(3)} q(x_j, t^n) \Delta x^3 + \mathcal{O}(\Delta x^4) \left. \right) - \alpha(x_{j-\frac{3}{2}}, t^n) \left( q(x_j, t^n) - \partial_x q(x_j, t^n) \Delta x \right. \\
& + \frac{1}{2} \partial^{(2)} q(x_j, t^n) \Delta x^2 - \frac{1}{6} \partial^{(3)} q(x_j, t^n) \Delta x^3 + \mathcal{O}(\Delta x^4) - q(x_j, t^n) \\
& \left. \left. + 2\partial_x q(x_j, t^n) \Delta x - 2\partial^{(2)} q(x_j, t^n) \Delta x^2 + \frac{4}{3} \partial^{(3)} q(x_j, t^n) \Delta x^3 + \mathcal{O}(\Delta x^4) \right) \right] \left. \right\} \\
= & \frac{\lambda \Delta t}{2\Delta x^2} \left\{ \partial_x q(x_j, t^n) \left[ \alpha(x_{j+\frac{1}{2}}, t^n) - 2\alpha(x_{j-\frac{1}{2}}, t^n) + \alpha(x_{j-\frac{3}{2}}, t^n) \right] \right. \\
& + \frac{1}{2} \partial_x^{(2)} q(x_j, t^n) \Delta x \left[ \alpha(x_{j+\frac{1}{2}}, t^n) + 2\alpha(x_{j-\frac{1}{2}}, t^n) - 3\alpha(x_{j-\frac{3}{2}}, t^n) \right] \\
& \left. + \frac{1}{6} \partial_x^{(3)} q(x_j, t^n) \Delta x^2 \left[ \alpha(x_{j+\frac{1}{2}}, t^n) - 2\alpha(x_{j-\frac{1}{2}}, t^n) + 7\alpha(x_{j-\frac{3}{2}}, t^n) \right] + \mathcal{O}(\Delta x^4) \right\} \\
= & \frac{\lambda \Delta t}{2} \left[ \partial_x q(x_j, t^n) \partial_x^{(2)} \alpha(x_j, t^n) + 2\partial_x^{(2)} q(x_j, t^n) \partial_x \alpha(x_j, t^n) \right. \\
& \left. + \partial_x^{(3)} q(x_j, t^n) \alpha(x_j, t^n) + \mathcal{O}(\Delta x) \right] \\
= & \frac{\lambda \Delta t}{2} \partial_x [\partial_x (\alpha(x_j, t^n) \partial_x q(x_j, t^n))] + \mathcal{O}(\Delta x \Delta t).
\end{aligned}$$

- Local truncation error contribution of the diffusion term:

$$-\frac{1}{\Delta x^2} \left\{ \bar{\alpha}(x_{j+\frac{1}{2}}, t^n) \left[ q(x_{j+1}, t^n) - q(x_j, t^n) \right] \right.$$

$$\begin{aligned}
& + \frac{\Delta t}{2} \left( -\lambda [q(x_{j+2}, t^n) - 2q(x_{j+1}, t^n) + q(x_j, t^n)] \right. \\
& + \frac{1}{\Delta x^2} \alpha(x_{j+\frac{3}{2}}, t^n) [q(x_{j+2}, t^n) - q(x_{j+1}, t^n)] \\
& - \frac{1}{\Delta x^2} \alpha(x_{j+\frac{1}{2}}, t^n) [2q(x_{j+1}, t^n) - 2q(x_j, t^n)] \\
& + \frac{1}{\Delta x^2} \alpha(x_{j-\frac{1}{2}}, t^n) [q(x_j, t^n) - q(x_{j-1}, t^n)] \\
& \left. + \beta [q(x_{j+1}, t^n) - q(x_j, t^n)] \right) \\
& + \bar{\alpha}(x_{j-\frac{1}{2}}, t^n) \left[ q(x_{j-1}, t^n) - q(x_j, t^n) \right. \\
& + \frac{\Delta t}{2} \left( -\lambda [-q(x_{j+1}, t^n) + 2q(x_j, t^n) - q(x_{j-1}, t^n)] \right. \\
& - \frac{1}{\Delta x^2} \alpha(x_{j+\frac{1}{2}}, t^n) [q(x_{j+1}, t^n) - q(x_j, t^n)] \\
& + \frac{1}{\Delta x^2} \alpha(x_{j-\frac{1}{2}}, t^n) [2q(x_j, t^n) - 2q(x_{j-1}, t^n)] \\
& - \frac{1}{\Delta x^2} \alpha(x_{j-\frac{3}{2}}, t^n) [q(x_{j-1}, t^n) - q(x_{j-2}, t^n)] \\
& \left. \left. + \beta [q(x_{j-1}, t^n) - q(x_j, t^n)] \right) \right] \Big\} \\
= & - [\partial_x \bar{\alpha}(x_j, t^n)] (\partial_x q(x_j, t^n)) - \frac{\bar{\alpha}(x_{j+1}, t^n) + \bar{\alpha}(x_{j-1}, t^n)}{2} \partial_x^{(2)} q(x_j, t^n) \\
& - \lambda \frac{\Delta t}{2} (\partial_x \bar{\alpha}(x_j, t^n)) \left( \partial_x^{(2)} q(x_j, t^n) \right) + \lambda \frac{\Delta t}{2} \bar{\alpha}(x_j, t^n) \left( \partial_x^{(3)} q(x_j, t^n) \right) \\
& - \frac{\Delta t}{2} \left[ (\partial_x q(x_j, t^n)) \left( \partial_x^{(2)} \alpha(x_j, t^n) \right) (\partial_x \bar{\alpha}(x_j, t^n)) \right. \\
& + \bar{\alpha}(x_j, t^n) (\partial_x q(x_j, t^n)) \left( \partial_x^{(3)} \alpha(x_j, t^n) \right) \\
& + 2 (\partial_x \bar{\alpha}(x_j, t^n)) \left( \partial_x^{(2)} q(x_j, t^n) \right) (\partial_x \alpha(x_j, t^n)) \\
& + 3 \bar{\alpha}(x_j, t^n) \left( \partial_x^{(2)} q(x_j, t^n) \right) \left( \partial_x^{(2)} \alpha(x_j, t^n) \right) \\
& + (\partial_x \bar{\alpha}(x_j, t^n)) \left( \partial_x^{(3)} q(x_j, t^n) \right) \alpha(x_j, t^n) \\
& + 3 \bar{\alpha}(x_j, t^n) \left( \partial_x^{(3)} q(x_j, t^n) \right) (\partial_x \alpha(x_j, t^n)) \\
& \left. + \bar{\alpha}(x_j, t^n) \left( \partial_x^{(4)} q(x_j, t^n) \right) \alpha(x_j, t^n) \right] - \beta \frac{\Delta t}{2} \left[ (\partial_x \bar{\alpha}(x_j, t^n)) (\partial_x q(x_j, t^n)) \right. \\
& \left. + \bar{\alpha}(x_j, t^n) \left( \partial_x^{(2)} q(x_j, t^n) \right) \right] + \mathcal{O}(\Delta x^2) + \mathcal{O}(\Delta x \Delta t) \\
= & -\partial_x (\alpha(x_j, t^n) \partial_x q(x_j, t^n)) + \frac{\Delta t}{2} \left\{ \partial_x (\partial_t \alpha(x_j, t^n) \partial_x q(x_j, t^n)) \right. \\
& - \lambda \partial_x \left( \alpha(x_j, t^n) \partial_x^{(2)} q(x_j, t^n) \right) + \partial_x \left[ \alpha(x_j, t^n) \partial_x^{(2)} (\alpha(x_j, t^n) \partial_x q(x_j, t^n)) \right] \\
& \left. + \beta \partial_x (\alpha(x_j, t^n) \partial_x q(x_j, t^n)) \right\} + \mathcal{O}(\Delta x^2) + \mathcal{O}(\Delta x \Delta t).
\end{aligned}$$

- Local truncation error contribution of the diffusion term to the source term:

$$-\frac{\beta \Delta t}{2 \Delta x^2} \left\{ \alpha(x_{j+\frac{1}{2}}, t^n) [q(x_{j+1}, t^n) - q(x_j, t^n)] \right.$$

$$\begin{aligned}
& -\alpha(x_{j-\frac{1}{2}}, t^n) [q(x_j, t^n) - q(x_{j-1}, t^n)] \Big\} \\
= & -\frac{\beta\Delta t}{2\Delta x^2} \left[ \alpha(x_{j+\frac{1}{2}}, t^n) \left( q(x_j, t^n) + \partial_x q(x_j, t^n)\Delta x + \frac{1}{2}\partial^{(2)}q(x_j, t^n)\Delta x^2 \right. \right. \\
& \left. \left. + \frac{1}{6}\partial^{(3)}q(x_j, t^n)\Delta x^3 + \mathcal{O}(\Delta x^4) - q(x_j, t^n) \right) \right. \\
& \left. - \alpha(x_{j-\frac{1}{2}}, t^n) \left( q(x_j, t^n) - q(x_{j-1}, t^n) - \partial_x q(x_j, t^n)\Delta x \right. \right. \\
& \left. \left. + \frac{1}{2}\partial^{(2)}q(x_j, t^n)\Delta x^2 - \frac{1}{6}\partial^{(3)}q(x_j, t^n)\Delta x^3 + \mathcal{O}(\Delta x^4) \right) \right] \\
= & -\frac{\beta\Delta t}{2\Delta x} \left[ \partial_x q(x_j, t^n) \left( \alpha(x_{j+\frac{1}{2}}, t^n) - \alpha(x_{j-\frac{1}{2}}, t^n) \right) \right. \\
& \left. + \frac{1}{2}\partial_x^2 q(x_j, t^n)\Delta x \left( \alpha(x_{j+\frac{1}{2}}, t^n) + \alpha(x_{j-\frac{1}{2}}, t^n) \right) \right. \\
& \left. + \frac{1}{6}\partial_x^3 q(x_j, t^n)\Delta x^2 \left( \alpha(x_{j+\frac{1}{2}}, t^n) - \alpha(x_{j-\frac{1}{2}}, t^n) \right) + \mathcal{O}(\Delta x^3) \right] \\
= & -\frac{\beta\Delta t}{2}\partial_x (\alpha(x_j, t^n)\partial_x q(x_j, t^n)) + \mathcal{O}(\Delta x^2) + \mathcal{O}(\Delta x\Delta t).
\end{aligned}$$

Gathering together the previous terms and the already obtained for the linear advection-reaction equation (A.1), we get

$$\begin{aligned}
\tau^n = & \partial_t q(x_j, t^n) + \lambda\partial_x q(x_j, t^n) - \partial_x [\alpha(x_j, t^n)\partial_x q(x_j, t^n)] - \beta q(x_j, t^n) \\
& + \frac{\Delta t}{2} \left[ \partial_t^{(2)} q(x_j, t^n) + \lambda\partial_x [-\lambda\partial_x q(x_j, t^n) + \beta q(x_j, t^n)] \right. \\
& \left. - \beta [-\lambda\partial_x q(x_j, t^n) + \beta q(x_j, t^n)] \right] - \frac{\Delta t}{2} \left\{ \partial_x [\partial_t \alpha(x_j, t^n)\partial_x q(x_j, t^n)] \right. \\
& \left. - \lambda\partial_x [\alpha(x_j, t^n)\partial_x^2 q(x_j, t^n)] + \partial_x \left\{ \alpha(x_j, t^n)\partial_x^2 [\alpha(x_j, t^n)\partial_x q(x_j, t^n)] \right\} \right. \\
& \left. + \beta\partial_x [\alpha(x_j, t^n)\partial_x q(x_j, t^n)] \right\} - \frac{\beta\Delta t}{2}\partial_x [\alpha(x_j, t^n)\partial_x q(x_j, t^n)] \\
& + \frac{\Delta t}{2}\partial_x^{(2)} [\alpha(x_j, t^n)\partial_x q(x_j, t^n)] + \mathcal{O}(\Delta t^2) + \mathcal{O}(\Delta x^2) + \mathcal{O}(\Delta x\Delta t) \\
= & \mathcal{O}(\Delta t^2) + \mathcal{O}(\Delta x^2) + \mathcal{O}(\Delta x\Delta t).
\end{aligned}$$

Where we have take into account that, following Cauchy-Kovalevskaya,

$$\begin{aligned}
& \partial_t^{(2)} q - \lambda^2 \partial_x^2 q - \partial_x \left[ \alpha \partial_x^{(2)} (\alpha \partial_x q) \right] - \beta^2 q + 2\lambda\beta\partial_x q - 2\beta\partial_x (\alpha\partial_x q) \\
& - \partial_x [(\partial_t \alpha) (\partial_x q)] + \lambda\partial_x^{(2)} (\alpha\partial_x q) + \lambda\partial_x (\alpha\partial_x^{(2)} q) = 0.
\end{aligned}$$

Thus, we conclude that the scheme is second order in space and time.